



Exotic Nuclei Studied by Direct Reactions at Low Momentum Transfer – Recent Results and Future Perspectives at FAIR



Peter Egelhof
GSI Darmstadt, Germany

Workshop on Advances in Nuclear Physics, ANUP 2011

Goa, India
November 7 – 8, 2011



Exotic Nuclei Studied by Direct Reactions at Low Momentum Transfer – Recent Results and Future Perspectives at FAIR



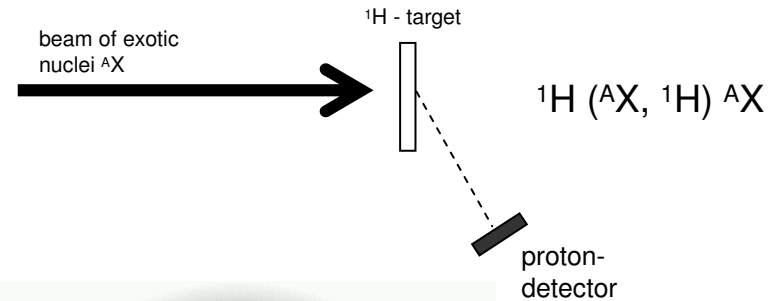
- I. Introduction
- II. Intermediate Energy Elastic Proton Scattering
- a Tool to Study the Radial Shape of Exotic Nuclei
- III. Recent Results on Halo Structures
in Exotic Be and C Isotopes
- IV. Perspectives at the Future Facility FAIR: The EXL Project*
- V. Conclusions

* EXL: EXotic Nuclei Studied in Light-Ion Induced Reactions at the NESR Storage Ring

I. Introduction

classical method of nuclear spectroscopy:

- ⇒ light ion induced direct reactions: (p,p), (p,p'), (d,p), ...
- ⇒ to investigate exotic nuclei: inverse kinematics
- ⇒ Important information at low momentum transfer



past and present experiments:

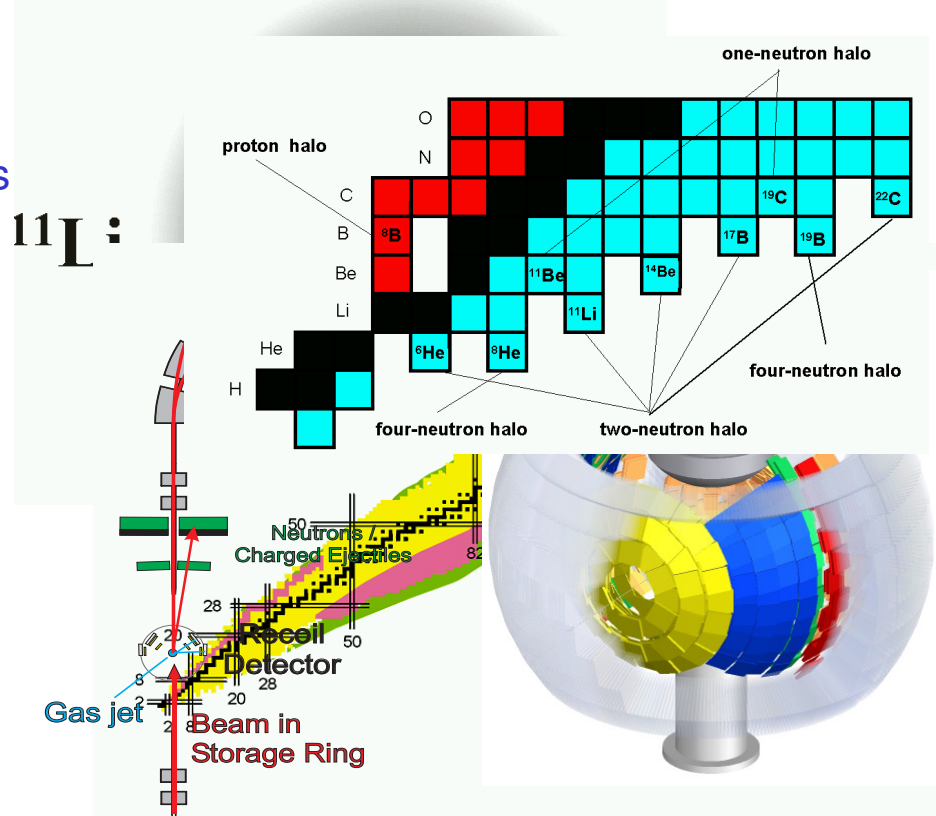
- ⇒ light neutron-rich nuclei: skin, halo structures
- ⇒ only at external targets
- ⇒ new technology: concept of active target

future perspectives at FAIR:

- ⇒ profit from intensity upgrade (up to 10^4 !!)
- ⇒ explore new regions of the chart of nuclides and new phenomena
- ⇒ use new and powerful methods:

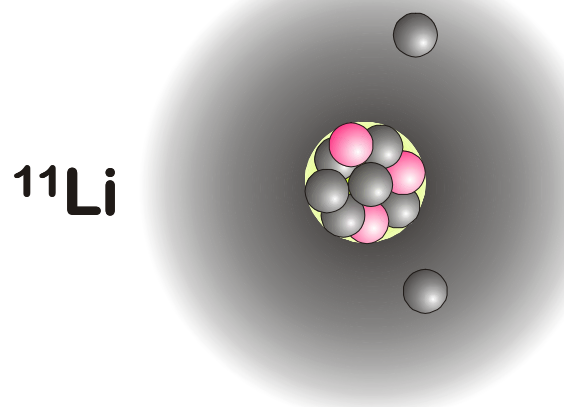
EXL: direct reactions at internal NESR target

- ⇒ high luminosity even for very low momentum transfer measurements

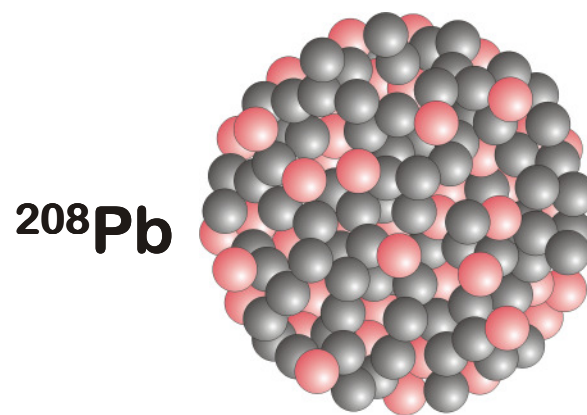


Halo-Nuclei – a New Phenomenon of the Structure of Nuclei

Density Distribution of Nuclear Matter

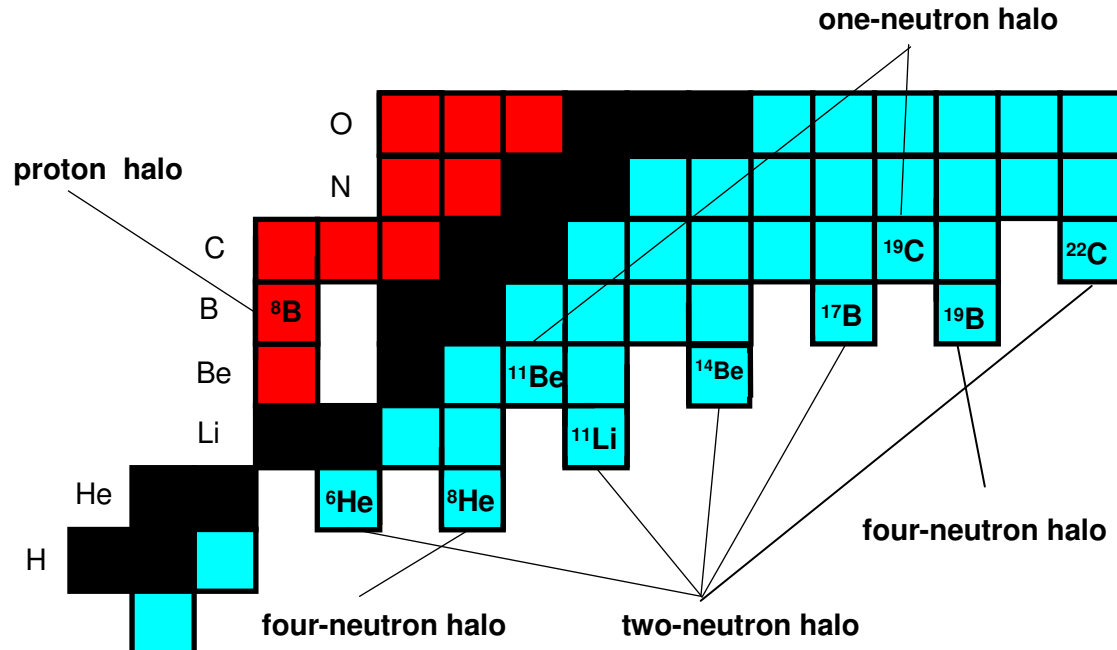


extremely neutron-rich nuclei:
neutron halo



stable nuclei:
neutrons and protons equally distributed

Reaction Experiments on Halo Nuclei



key reaction facility FAIR:

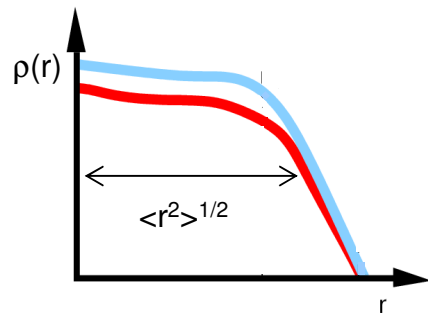
- total absorption cross section
- explore new regions of the chart of nuclides
- breakup reactions, knock-out reactions, transfer reactions
- elastic, inelastic scattering
- size and shape of matter distributions
→ discovery of halo (skin) structure
- internal targets at storage rings
- single particle (few body) structure
- resonant states beyond the dripline

new information:

II. Intermediate Energy Elastic Proton Scattering - a Tool to Study the Radial Shape of Exotic Nuclei

The radial shape and size of nuclei is a basic nuclear property !

⇒ of high interest for nuclear structure physics



observables: nuclear charge distribution: $\rho_{ch}(r), \langle r_{ch}^2 \rangle^{1/2}$ ⇒ leptonic probes
nuclear matter distribution: $\rho_m(r), \langle r_m^2 \rangle^{1/2}$ ⇒ hadronic probes

method: intermediate energy elastic proton scattering

- ⇒ well established method for determination of nuclear matter distributions (of stable nuclei)
- ⇒ what about exotic nuclei?



Intermediate Energy Elastic Proton Scattering - a Tool to Study the Radial Shape of Halo Nuclei

aim: quantitative information on the nuclear matter distributions

method: intermediate energy (700 – 1000 MeV) elastic proton scattering

of special interest: light isotopes with halo-structure: ^6He , ^8He , ^{11}Li , ^{14}Be , ^8B , $^{17}\text{C}(?)$

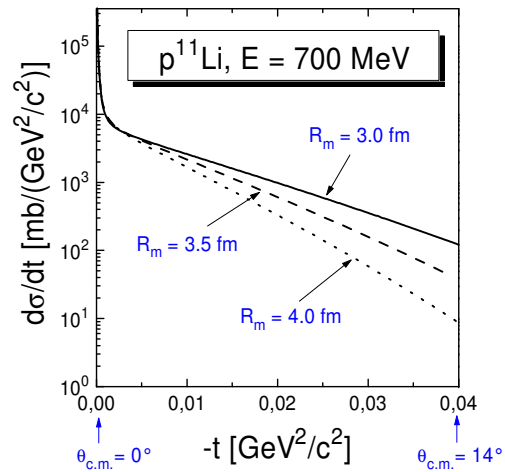
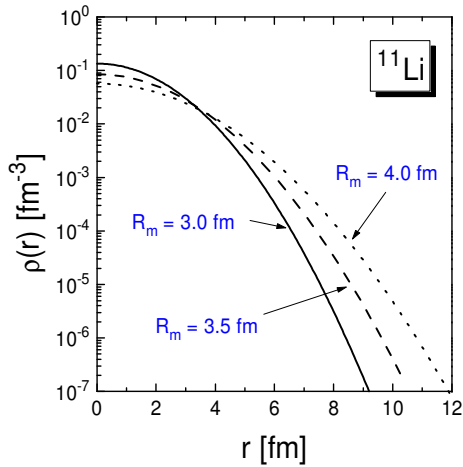
for low momentum transfer:

high sensitivity on the halo structure

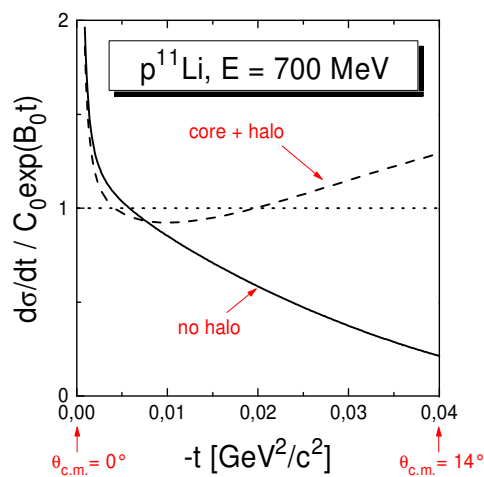
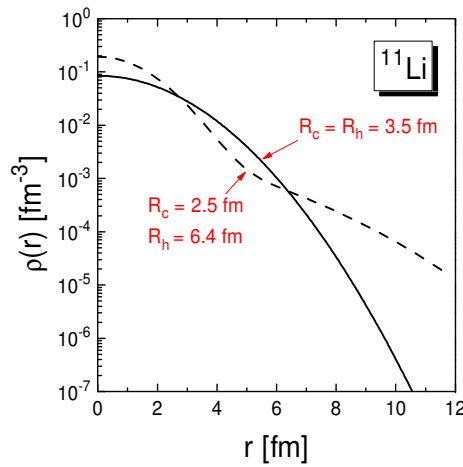
⇒ determination of matter radii

⇒ determination of the radial shape of the
nuclear matter distribution

Sensitivity of Elastic Proton Scattering on the Radial Shape of the Nuclear Matter Distribution



slope of $d\sigma/dt$
 \rightarrow matter radius R_m

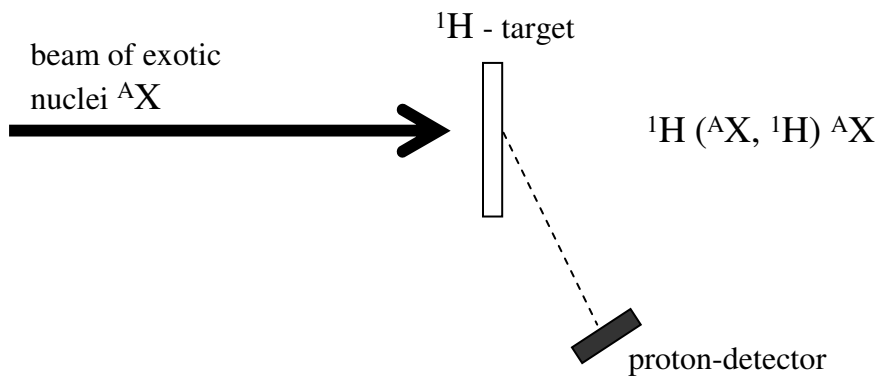


curvature of $\log(d\sigma/dt)$
 \rightarrow halo structure

Experiments at Low Momentum Transfer

experimental conditions:

- investigation of exotic nuclei
⇒ method of “Inverse Kinematics”



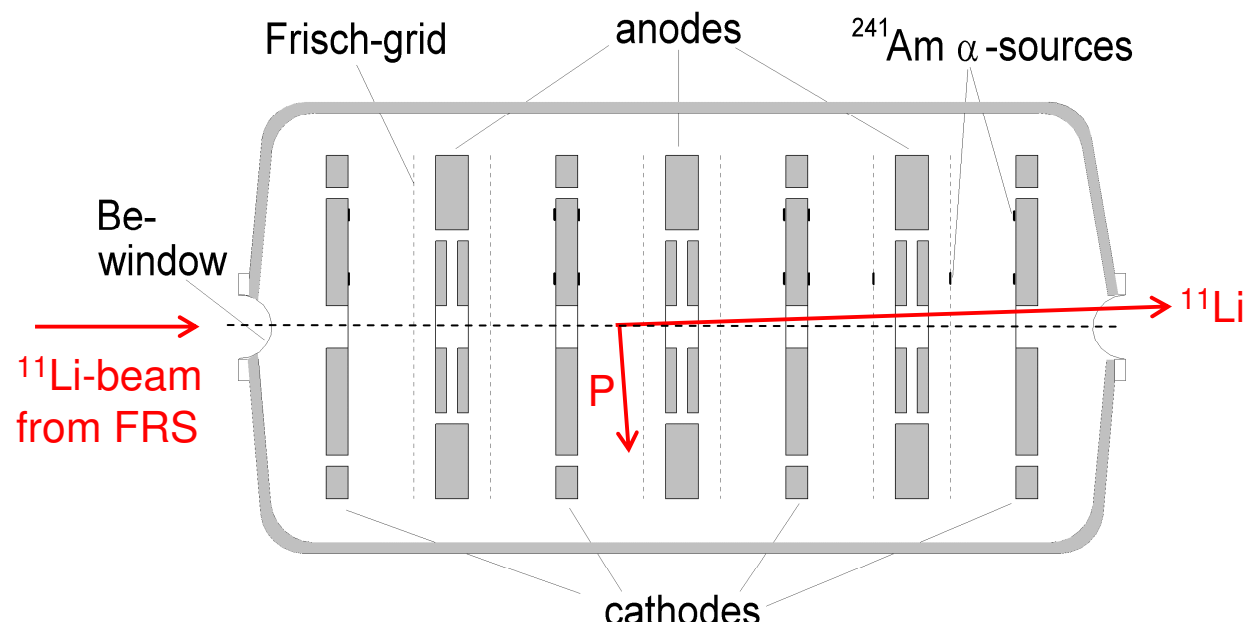
- high incident energies ($E = 700 \text{ MeV/u}$)
⇒ produce beam of exotic nuclei by projectile fragmentation at GSI:
Fragment Separator FRS
- low beam intensities: $10^2 - 10^4 \text{ sec}^{-1}$
- low recoil energies: $T_R \leq 10 \text{ MeV}$
⇒ needs thin target and large solid angle detector
solution: recoil detector “IKAR” as active target

The TPC-Ionization Chamber IKAR as Active Target

(provided by PNPI St. Petersburg)

detection principle:

H₂-target = detector for recoil protons



operating conditions:

H₂-pressure: 10 atm

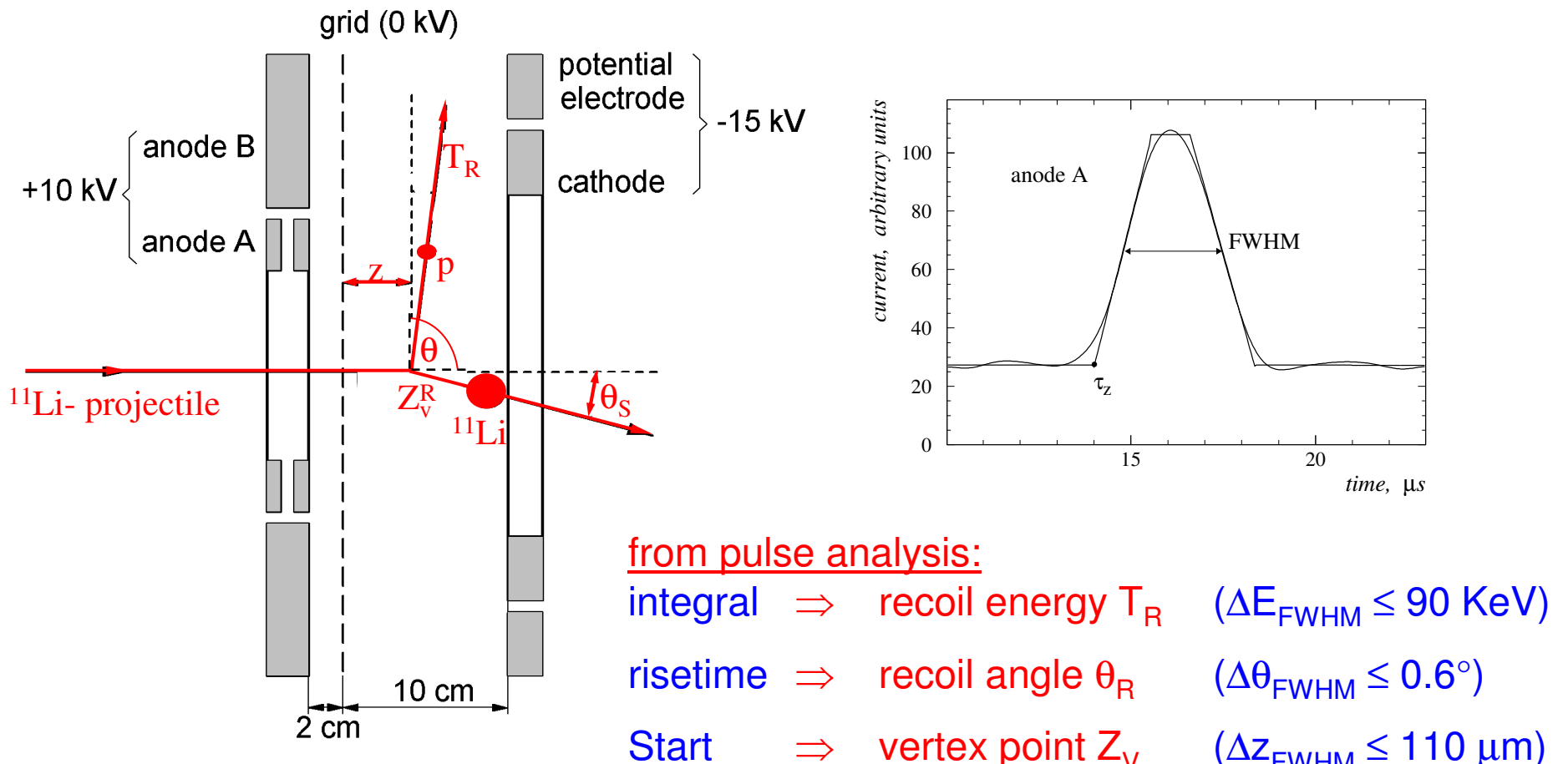
entrance window: 0.5 mm Beryllium

target thickness: 30 mg/cm² (6 independent sections)

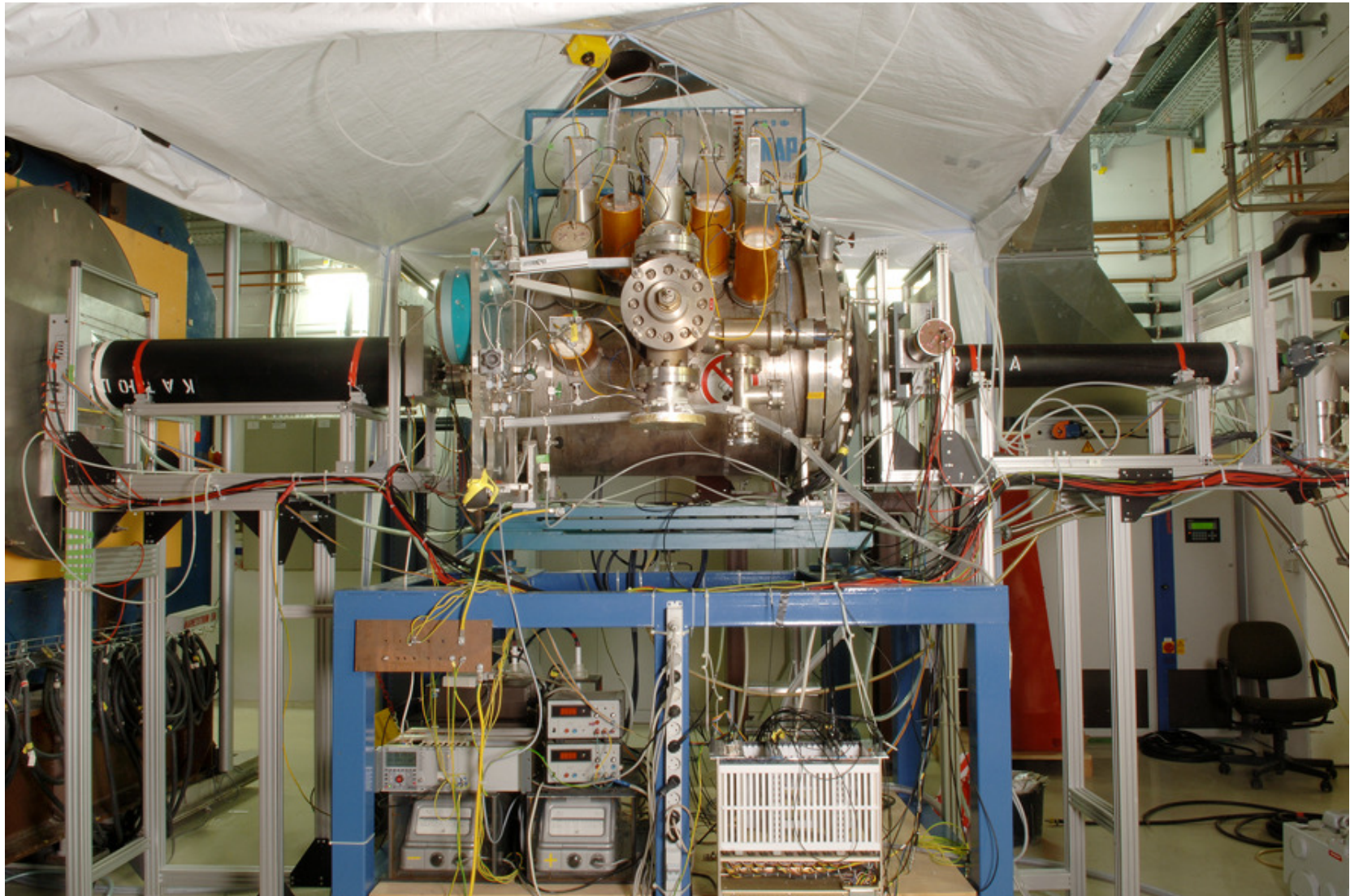
beam rate: $\leq 10^4/\text{sec}$

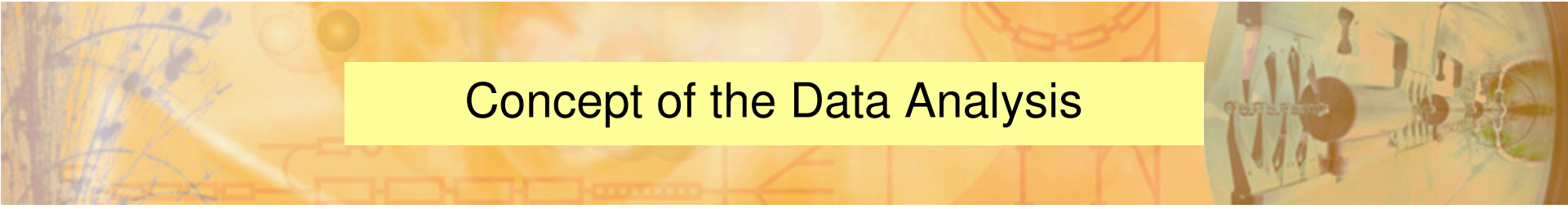
but: method limited to $Z \leq 6$!

Detection Principle of IKAR



The IKAR Experimental Setup





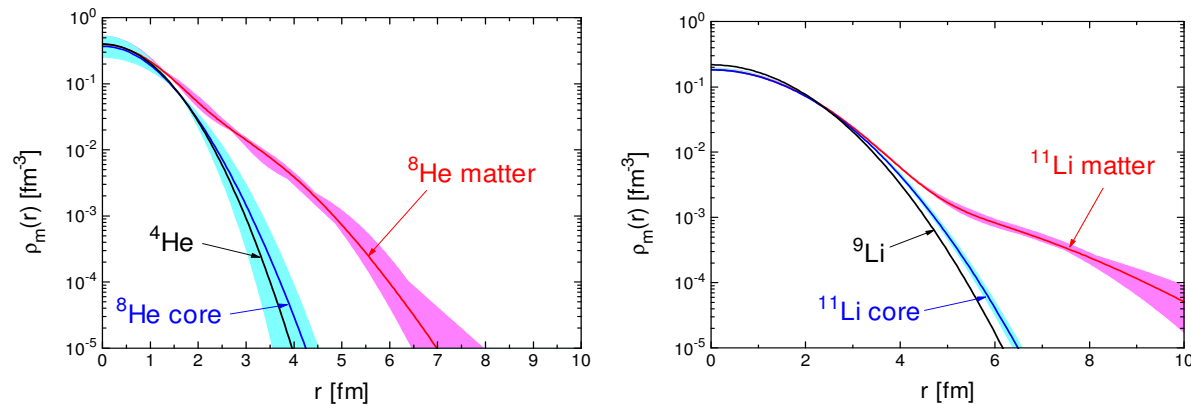
Concept of the Data Analysis

- Glauber multiple-scattering theory for calculation of cross sections:
 - use measured free pp, pn-cross sections as input (in medium effects negligible)
 - fold with nucleon density distribution
 - take into account multiple scattering (all terms!) (small for region of nuclear halo!)
- variation of the nucleon density distribution:
 - a) phenomenological parametrizations (point matter densities):
 - G: 1 Gaussian
 - SF: Symmetrized Fermi
 - GG: 2 Gaussians
 - GO: Gaussian + Harmonic Oscillator
 - b) “model independent” analysis:
 - SOG: Sum Of Gaussians

(standard method for electron scattering data:
I. Sick, Nucl. Phys. A 218 (1974) 509)

Investigation of Nuclear Matter Density Distributions of Halo Nuclei by Elastic Proton Scattering at Low Momentum Transfer

nuclear matter distributions:



nuclear matter radii:

nucleus	R_{matter} , fm	R_{core} , fm	R_{halo} , fm
^4He	1.49 (3)	--	--
^8He	2.53(8)	1.55 (15)	3.22 (14)
^9Li	2.44 (6)	--	--
^{11}Li	3.71 (20)	2.53 (3)	6.85 (58)

- extended neutron distribution in ^8He and ^{11}Li obtained
- size of core, halo and total matter distribution determined with high accuracy
- the picture of a ^9Li (^4He) core + 2 (4) valence neutron-structure is confirmed for ^{11}Li and ^8He

Determination of Neutron Radii and Neutron Skin Sizes

- needs input on proton (charge) distributions

⇒ use data from laser spectroscopy (isotope shift measurements):

for ${}^6\text{He}$: L.-B. Wang et al., PRL 93, 142501 (2004)

for ${}^{8,9,11}\text{Li}$: R. Sanchez et al., PRL 96, 033002 (2006)

M. Puchalski et al., PRL 97, 1330016 (2006)

- neutron radius:

$$R_n^2 = \frac{1}{N_n} * (A R_m^2 - N_p R_p^2)$$

- neutron skin size:

$$\delta_{np} = R_n - R_p$$

Summary of all Data on Nuclear Radii

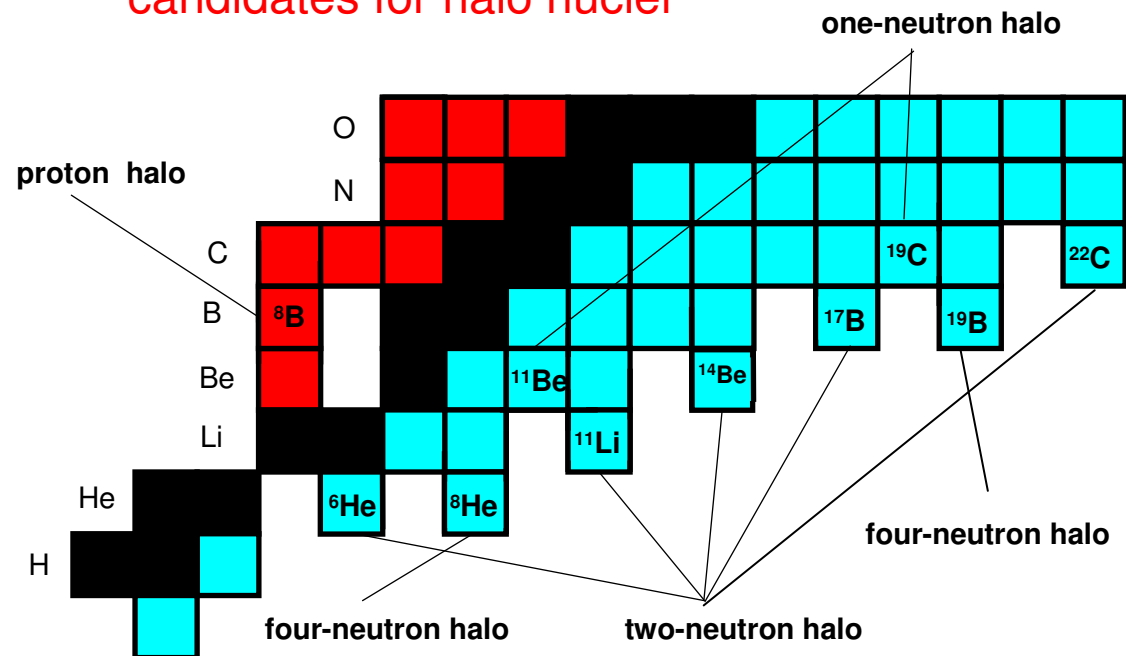
nucleus	R_m , fm	R_{core} , fm	R_{halo} , fm	R_p^* , fm	R_n , fm	δ_{np} , fm
${}^6\text{He}$	2.45 (10)	1.88 (12)	3.31 (28)	1.91 (2)	2.60 (7)	0.69 (7)
${}^8\text{Li}$	2.50 (6)	--	--	2.15 (3)	2.69 (9)	0.54 (10)
${}^9\text{Li}$	2.44 (6)	--	--	2.06 (4)	2.61 (9)	0.55 (10)
${}^{11}\text{Li}$	3.71 (20)	2.55 (12)	6.85 (58)	2.33(4)	3.75 (15)	1.42 (16)

* R_p from laser spectroscopy, unfolded from proton charge radius

III. Recent Results on Halo Structures in Exotic Be and C Isotopes

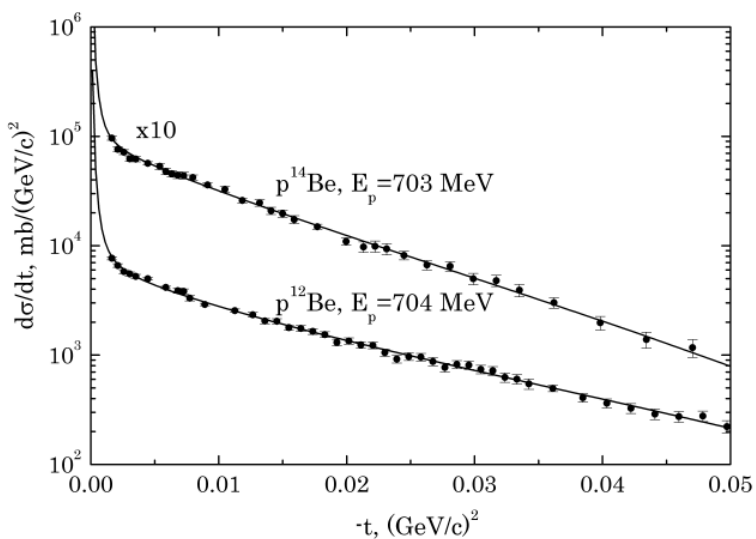
- two experiments with primary ^{12}C and ^{18}O beams were successfully performed
- data on ^{12}Be , ^{14}Be and ^{8}B , ^{15}C , ^{17}C were taken: S.Ilieva et al., S. Tang et al.

candidates for halo nuclei

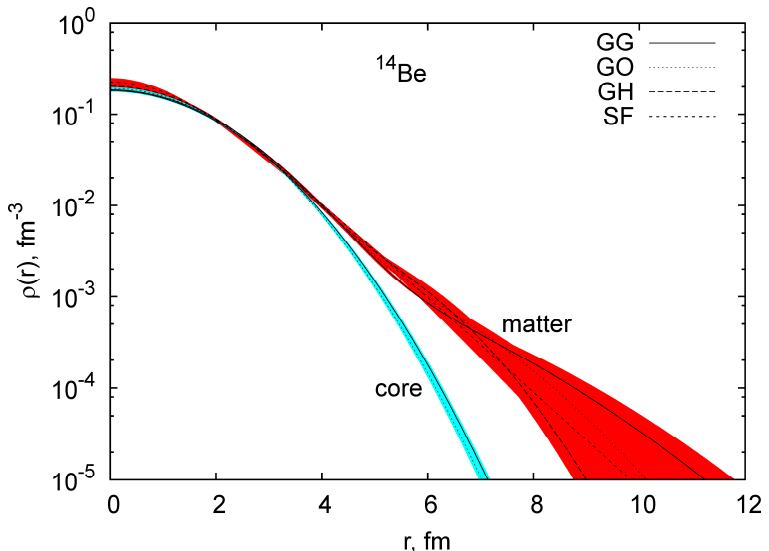


Elastic Proton Scattering from ^{14}Be

differential cross section:



deduced nuclear matter distribution:



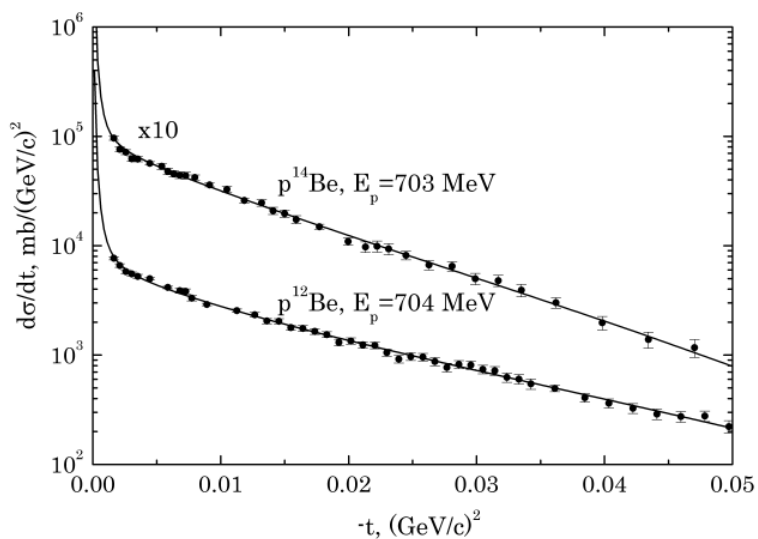
results for ^{14}Be :

$$\begin{aligned} R_{\text{matter}} &= 3.25 \pm 0.04 \pm 0.11 \text{ fm} \\ R_{\text{core}} &= 2.65 \pm 0.02 \pm 0.11 \text{ fm} \end{aligned}$$

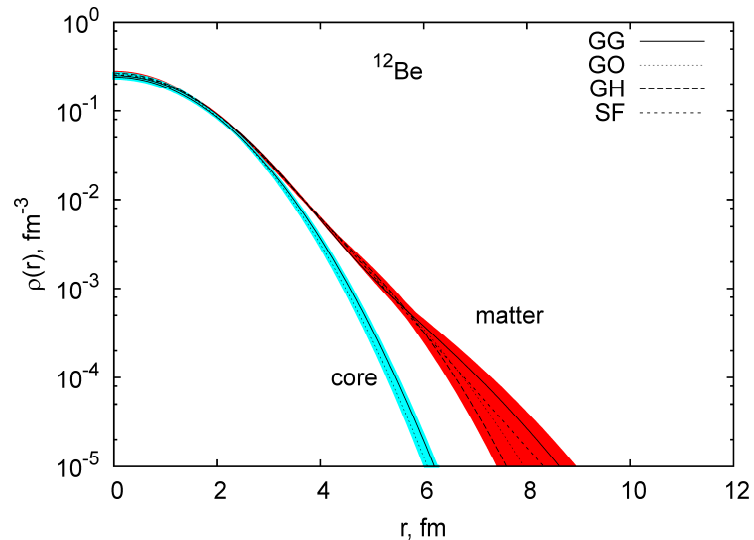
- ^{14}Be exhibits a pronounced core-halo structure
- the picture of a ^{12}Be -core + 2 valence neutron structure is confirmed
- the present data favour a relatively large s-wave component
(see I. Thompson et. al, Phys. Rev. C53 (1996) 708)

Elastic Proton Scattering from ^{12}Be

differential cross section:



deduced nuclear matter distribution:



results for ^{12}Be :

$$R_{\text{matter}} = 2.71 \pm 0.03 \pm 0.06 \text{ fm}$$

$$R_{\text{core}} = 2.17 \pm 0.02 \pm 0.09 \text{ fm}$$

- ^{12}Be exhibits an extended matter distribution
- the contribution of (sd) intruder states is confirmed
(see I. Thompson et al., Phys. Rev. C53 (1996) 703)



The IKAR-Collaboration

F. Aksouh, G.D. Alkhazov, M.N. Andronenko, L. Chulkov, A.V. Dobrovolsky,
P. Egelhof, H. Geissel, M. Gorska, S. Ilieva, A. Inglessi, A.V. Khanzadeev,
O. Kiselev, G.A. Korolev, C. L. Le, Y. Litvinov, G. Münzenberg, M. Mutterer,
S.R. Neumaier, C. Nociforo, C. Scheidenberger, L. Sergeev, D.M. Seliverstov,
H. Simon, S. Tang, N.A. Timofeev, A.A. Vorobyov, V. Volkov, H. Weick,
V.I. Yatsoura, A. Zhdanov

Gesellschaft für Schwerionenforschung, Darmstadt, Germany

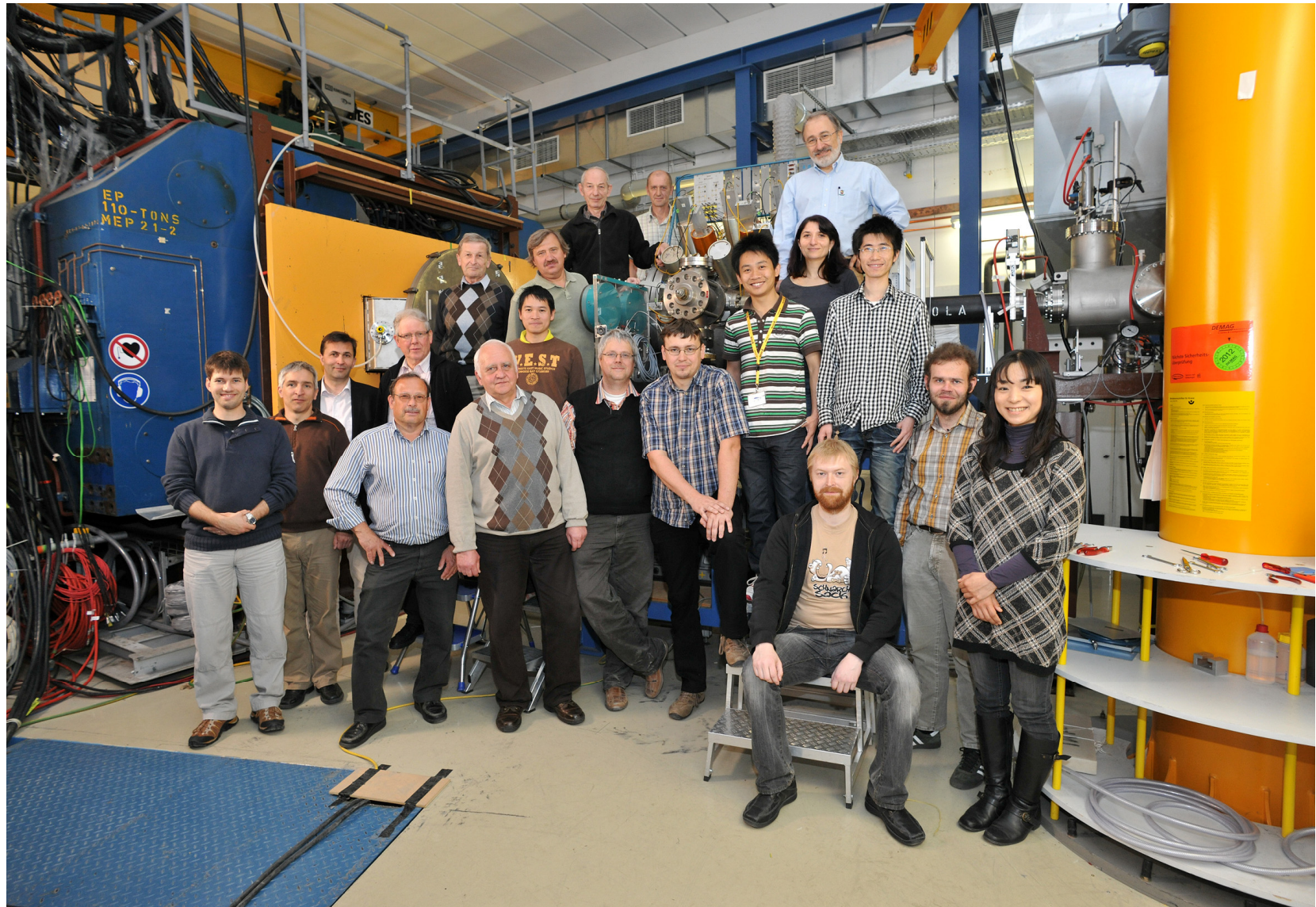
Petersburg Nuclear Physics Institute, Gatchina, Russia

Kurchatov Institute, Moscow, Russia

Institut für Kernchemie, Universität Mainz, Germany

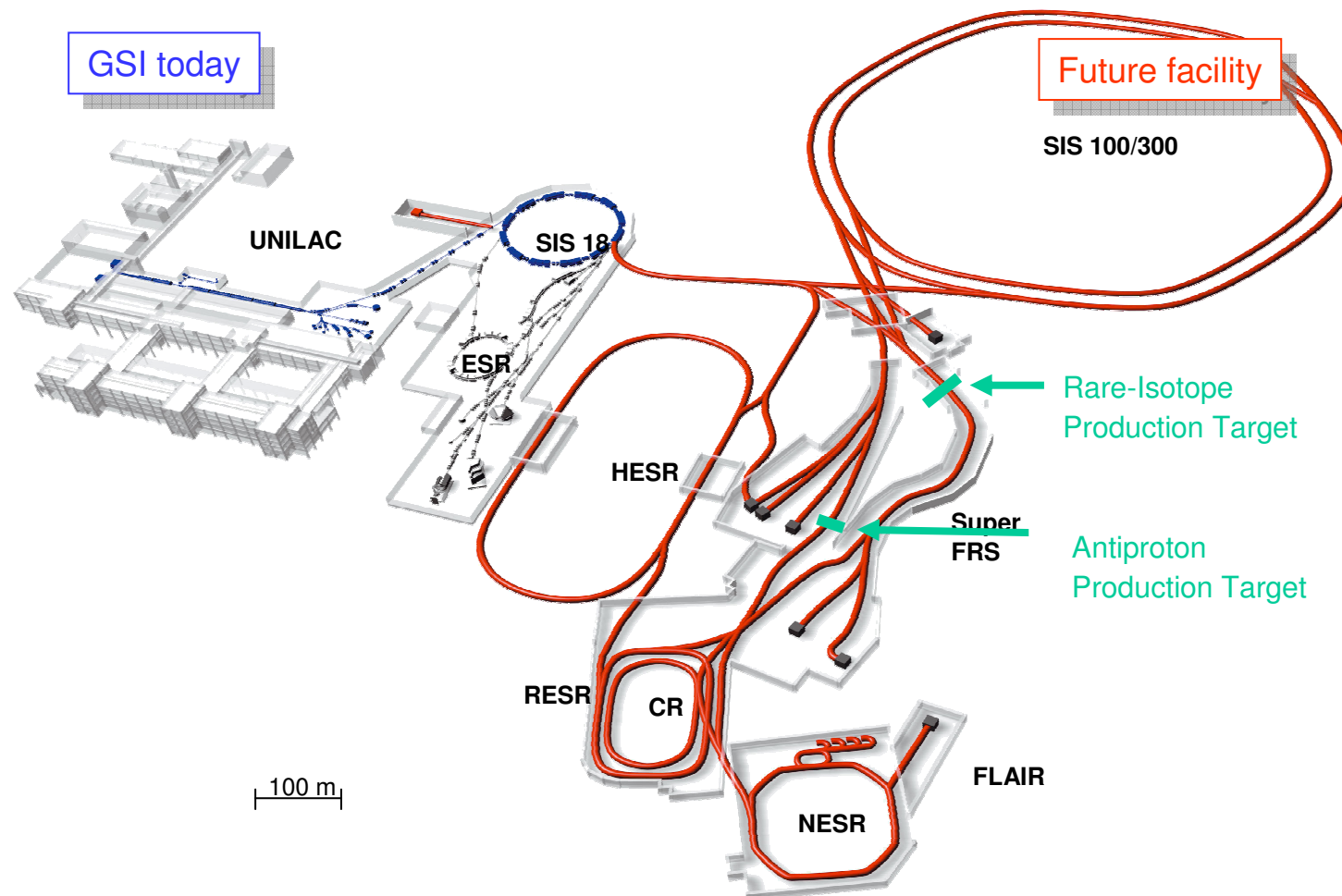
Institut für Kernphysik, TU Darmstadt, Darmstadt, Germany

The IKAR Collaboration

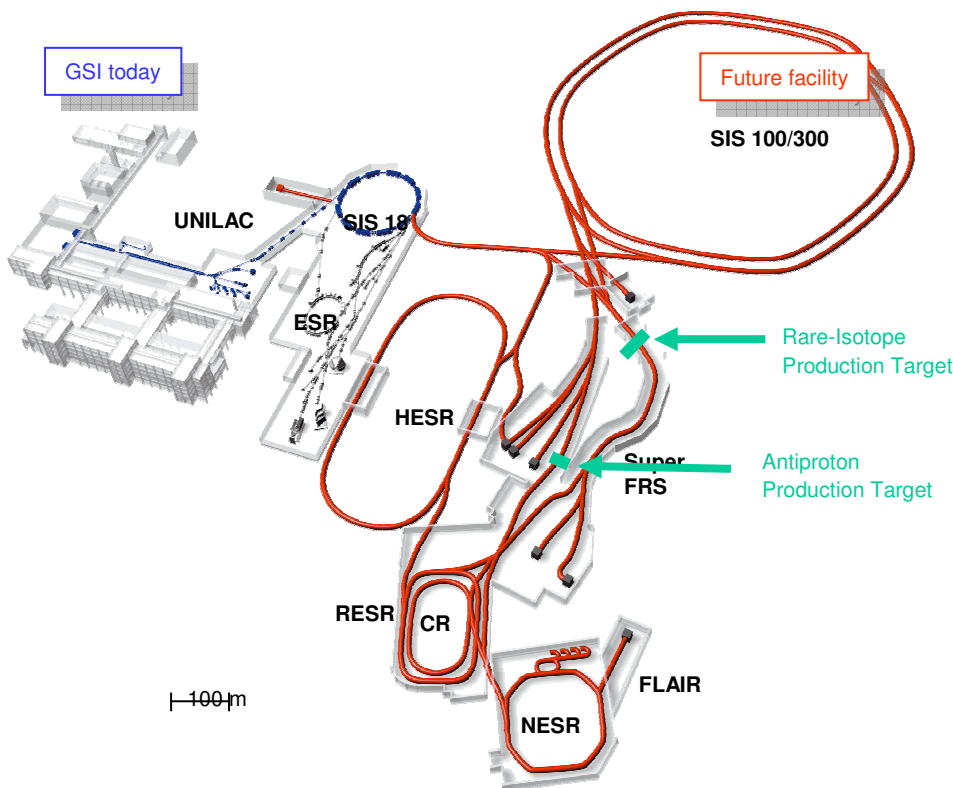


IV: Perspectives at the Future Facility FAIR: The EXL Project

FAIR: Facility for Antiproton and Ion Research



FAIR: Facility Characteristics



Key Technical Features

- Cooled beams
- Rapidly cycling superconducting magnets

Primary Beams

- $10^{12}/\text{s}$; 1.5-2 GeV/u; $^{238}\text{U}^{28+}$
- Factor 100-1000 over present in intensity
- $2(4)\times 10^{13}/\text{s}$ 30 GeV protons
- $10^{10}/\text{s}$ $^{238}\text{U}^{73+}$ up to 35 GeV/u
- up to 90 GeV protons

Secondary Beams

- Broad range of radioactive beams up to 1.5 - 2 GeV/u; up to factor 10 000 in intensity over present
- Antiprotons 3 - 30 GeV

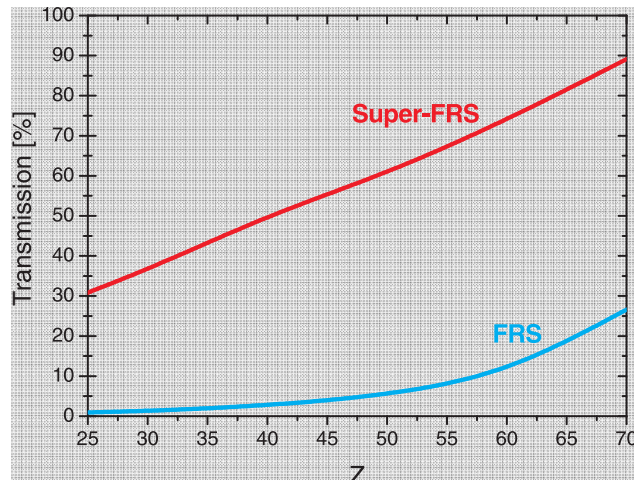
Storage and Cooler Rings

- Radioactive beams
- e – A collider
- 10^{11} stored and cooled 0.8 - 14.5 GeV antiprotons

Nuclear Physics with Radioactive Beams at FAIR: NUSTAR: NUclear STructure, Astrophysics and Reactions

I High intensity primary beams

from SIS 100 (e.g. $10^{12} \text{ }^{238}\text{U}$ / sec at 1 GeV/u)



Pre-Separator

II Superconducting
large acceptance
Fragmentseparator

Optimized for
efficient transport
of fission products

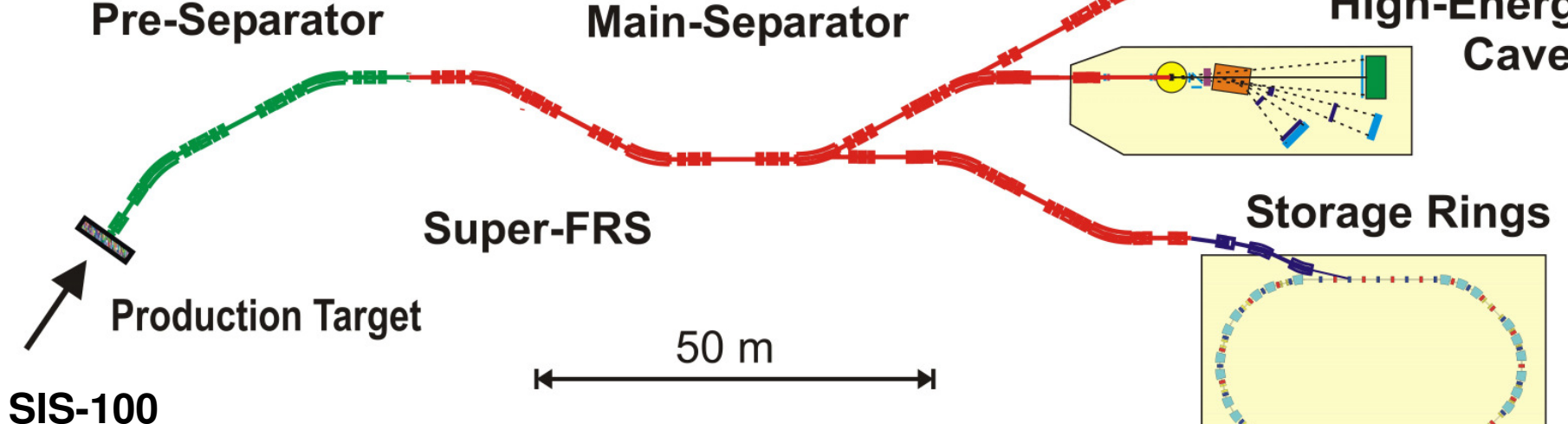
III Three experimental areas



Low-Energy
Cave



High-Energy
Cave



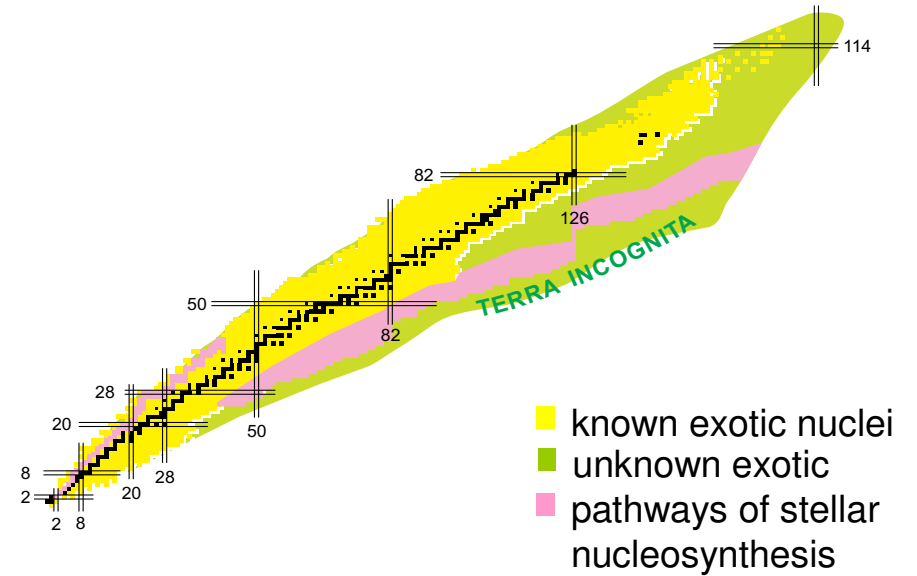
Perspectives at the GSI Future Facility FAIR

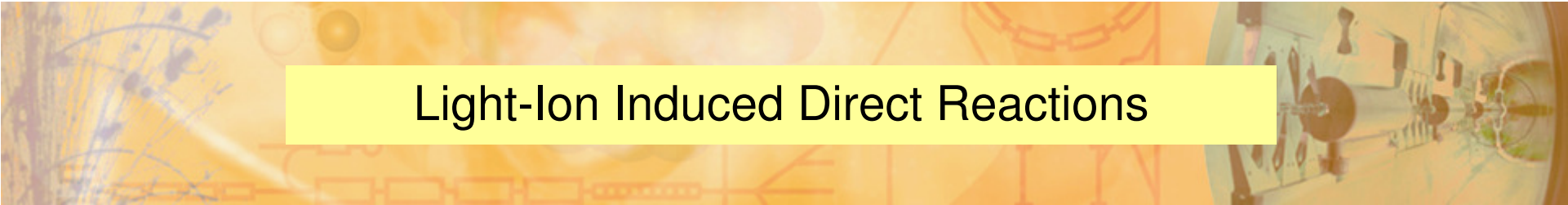
regions of interest:

⇒ towards the driplines for medium heavy and heavy nuclei

physics interest:

- matter distributions (halo, skin...)
- single-particle structure evolution (new magic numbers, new shell gaps, spectroscopic factors)
- NN correlations, pairing and clusterization phenomena
- new collective modes (different deformations for p and n, giant resonance strength)
- parameters of the nuclear equation of state
- in-medium interactions in asymmetric and low-density matter
- astrophysical r and rp processes, understanding of supernovae





Light-Ion Induced Direct Reactions

- elastic scattering (p,p), (α,α), ...
nuclear matter distribution $\rho(r)$, skins, halo structures
- inelastic scattering (p,p'), (α,α'), ...
deformation parameters, $B(E2)$ values, transition densities, giant resonances
- charge exchange reactions (p,n), ($^3\text{He},t$), ($d, ^2\text{He}$), ...
Gamow-Teller strength
- transfer reactions (p,d), (p,t), ($p, ^3\text{He}$), (d,p), ...
single particle structure, spectroscopic factors
spectroscopy beyond the driplines
neutron pair correlations
neutron (proton) capture cross sections
- knock-out reactions ($p,2p$), (p,pn), (p,p ^4He)...
ground state configurations, nucleon momentum distributions, cluster correlations

Reactions with Relativistic Radioactive Beams at FAIR

- R³B: Reactions with Relativistic Radioactive Beams
⇒ High Energy Branch
- EXL: EXotic Nuclei Studied in Light-Ion Induced Reactions at the NESR Storage Ring
⇒ Ring Branch
- ELISe: Electron Ion Scattering in a Storage Ring e-A Collider
⇒ Ring Branch

R3B: Reactions with Relativistic Radioactive Beams

The setup

Exotic beam from Super-FRS

γ -rays
Neutrons
Protons

Large-acceptance
dipole

Large-acceptance measurement

Protons

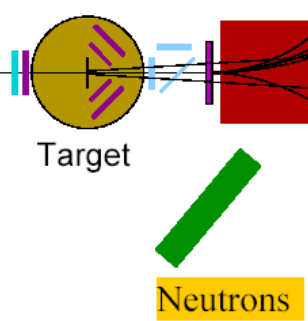
Heavy fragments

R³B

Neutrons



Tracking detectors:
 ΔE , x , y , ToF, $B\rho$



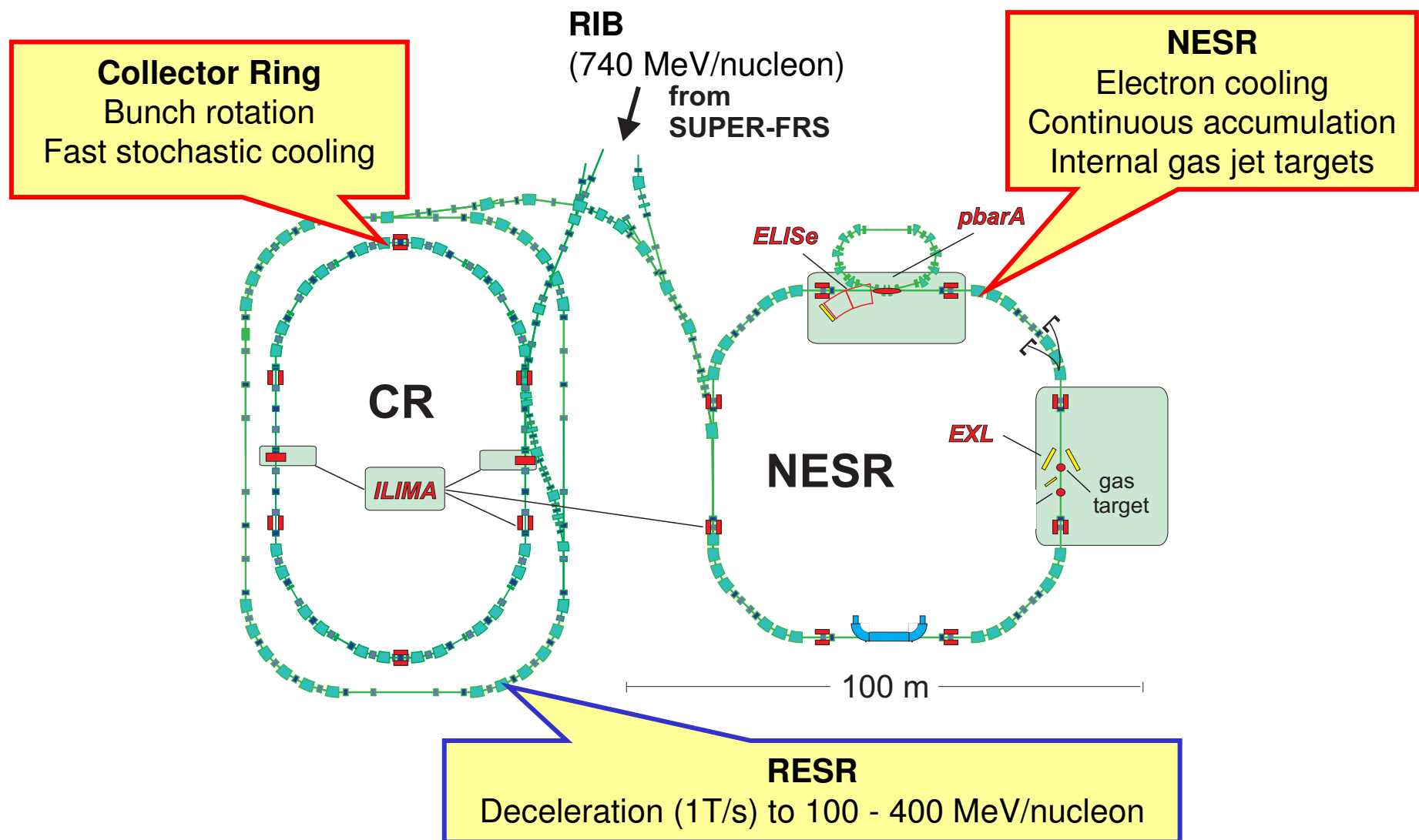
Target

High-resolution measurement

Neutrons

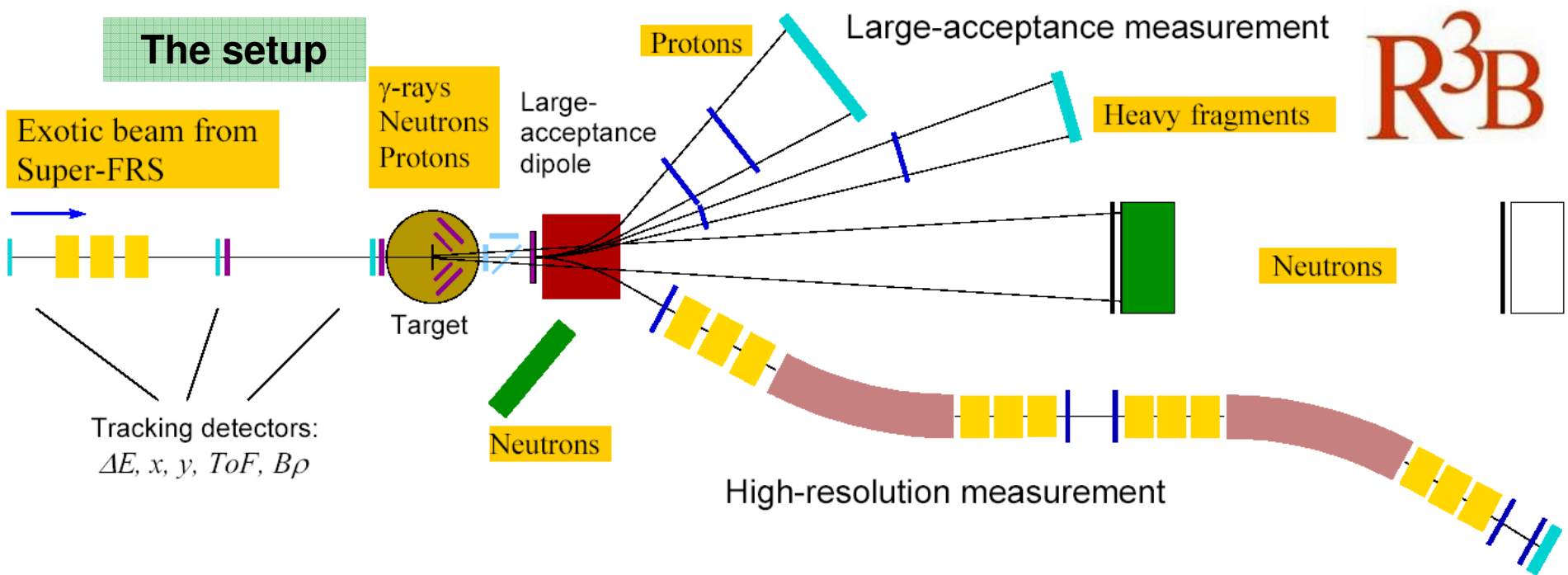
The R³B experiment: a universal setup for kinematical complete measurements

Experiments with Stored Exotic Nuclei



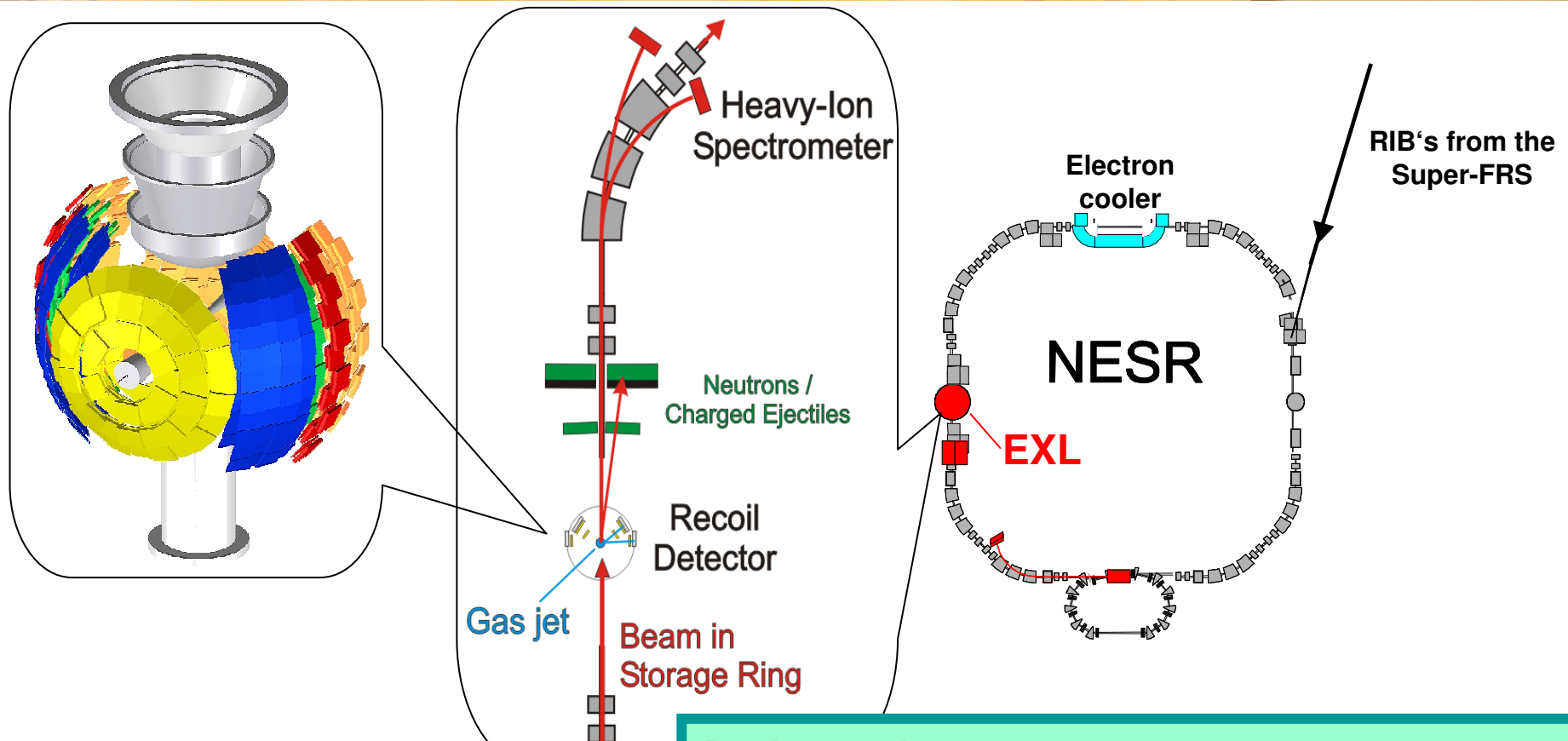
R3B: Reactions with Relativistic Radioactive Beams

The setup



The R³B experiment: a universal setup for kinematical complete measurements

EXL: EXotic Nuclei Studied in Light-Ion Induced Reactions at the NESR Storage Ring



Detection systems for:

- Target recoils and gammas (p, α, n, γ)
- Forward ejectiles (p, n)
- Beam-like heavy ions

Design goals:

- Universality: applicable to a wide class of reactions
- High energy resolution and high angular resolution
- Large solid angle acceptance
- Specially dedicated for low q measurements with high luminosity ($> 10^{29} \text{ cm}^{-2} \text{ s}^{-1}$)

Light-Ion Induced Direct Reactions at Low Momentum Transfer

- elastic scattering (p,p), (α,α), ...
nuclear matter distribution $\rho(r)$, skins, halo structures
- inelastic scattering (p,p'), (α,α'), ...
deformation parameters, $B(E2)$ values, transition densities, giant resonances
- transfer reactions (p,d), (p,t), ($p, {}^3\text{He}$), (d,p), ...
single particle structure, spectroscopic factors, spectroscopy beyond the driplines,
neutron pair correlations, neutron (proton) capture cross sections
- charge exchange reactions (p,n), (${}^3\text{He},t$), ($d, {}^2\text{He}$), ...
Gamow-Teller strength
- knock-out reactions ($p,2p$), (p,pn), ($p,p {}^4\text{He}$)...
ground state configurations, nucleon momentum distributions

for almost all cases:

region of low momentum transfer
contains most important information

Speciality of EXL:

measurements at very low momentum transfer
⇒ complementary to R³B !!!

Experiments to be Performed at Very Low Momentum Transfer – Some Selected Examples

- Investigation of Nuclear Matter Distributions:

- ⇒ halo, skin structure
- ⇒ probe in-medium interactions at extreme isospin (almost pure neutron matter)
- ⇒ in combination with electron scattering (ELISe project @ FAIR):
separate neutron/proton content of nuclear matter (deduce neutron skins)

method: elastic proton scattering ⇒ at low q: high sensitivity to nuclear periphery

- Investigation of the Giant Monopole Resonance:

- ⇒ gives access to nuclear compressibility ⇒ key parameters of the EOS
- ⇒ new collective modes (breathing mode of neutron skin)

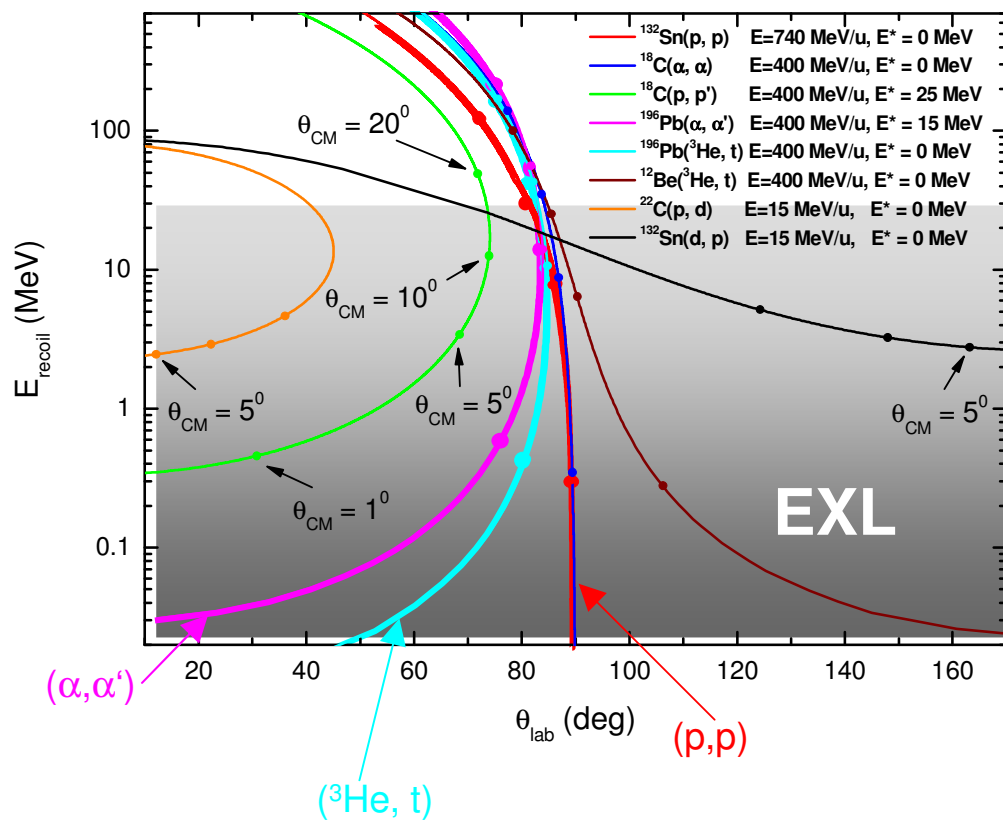
method: inelastic α scattering at low q

- Investigation of Gamow-Teller Transitions:

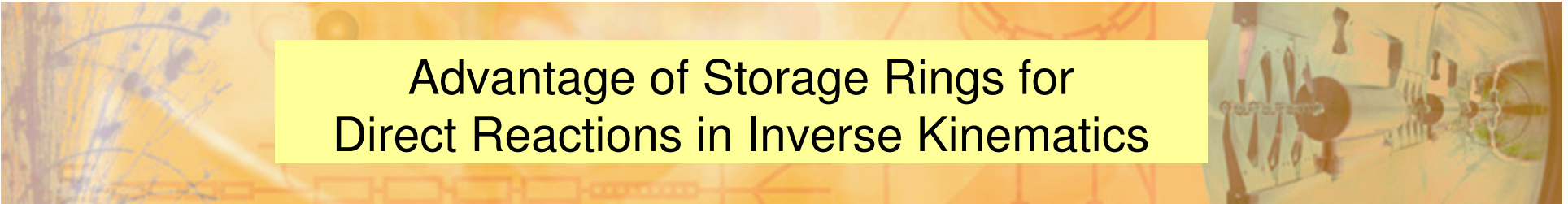
- ⇒ weak interaction rates for $N = Z$ waiting point nuclei in the rp-process
- ⇒ electron capture rates in the presupernova evolution (core collaps)

method: ($^3\text{He}, t$), ($d, ^2\text{He}$) charge exchange reactions at low q

Kinematical Conditions for Light-Ion Induced Direct Reactions in Inverse Kinematics



- required beam energies:
 $E \approx 200 \dots 740$ MeV/u
(except for transfer reactions)
- required targets: $^{1,2}\text{H}$, $^{3,4}\text{He}$
- most important information in region of low momentum transfer
⇒ low recoil energies of recoil particles
⇒ need thin targets for sufficient angular and energy resolution



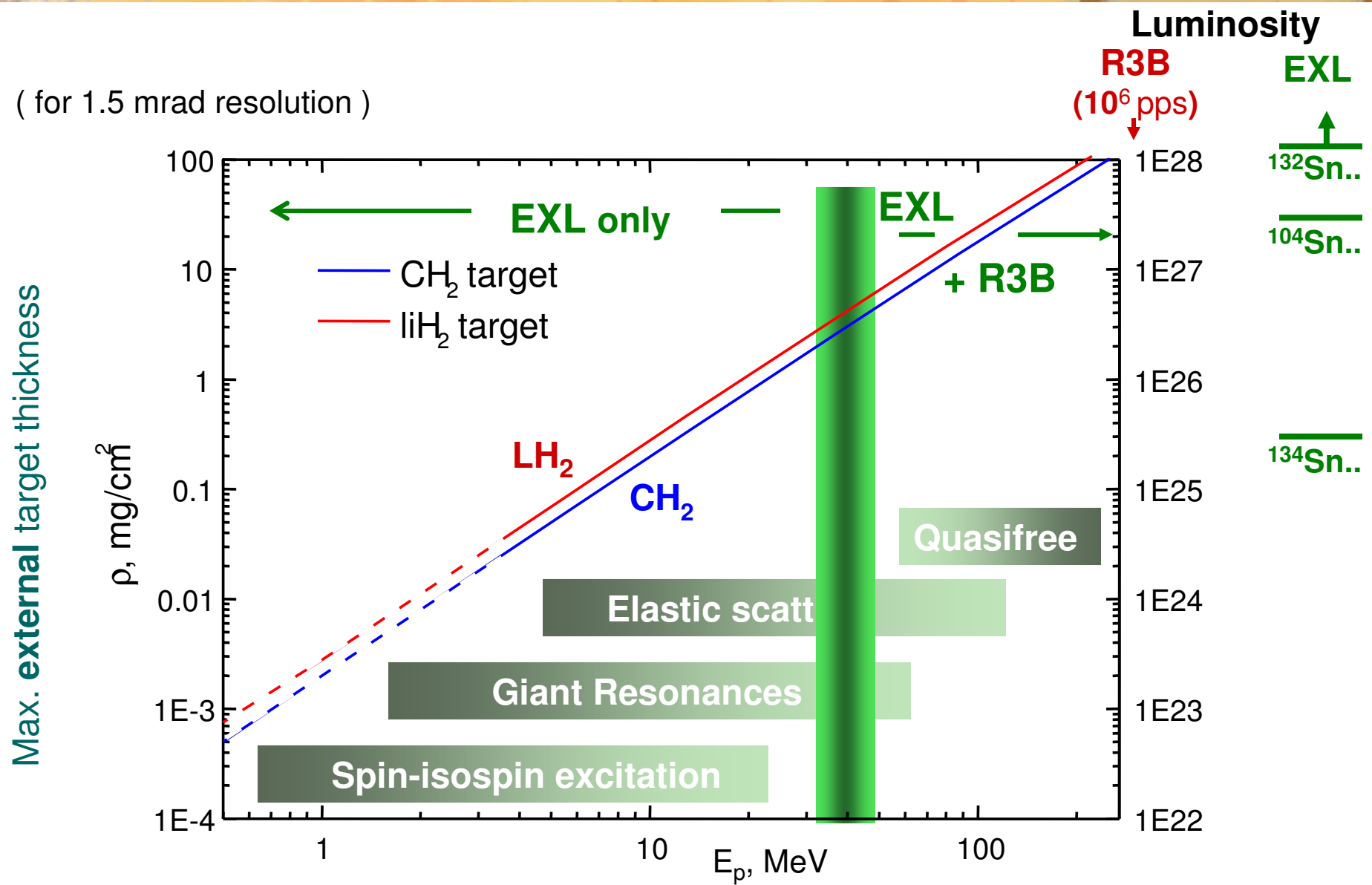
Advantage of Storage Rings for Direct Reactions in Inverse Kinematics

- low threshold and high resolution due to: beam cooling, thin target (10^{14} - 10^{15} cm $^{-2}$)
- gain of luminosity due to: continuous beam accumulation and recirculation
- low background due to: pure, windowless $^{1,2}\text{H}_2$, $^{3,4}\text{He}$, etc. targets
- experiments with isomeric beams

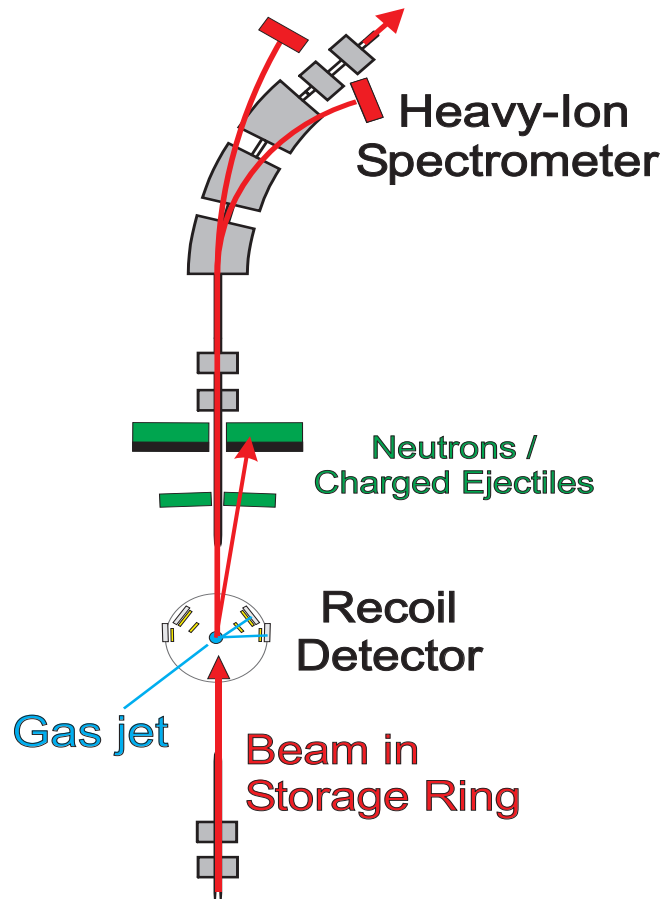
Experiments at very low momentum transfer can only be done at EXL
(except with ACTAR, but with lower luminosity)

Only the world-wide unique combination of Super-FRS and NESR provides high resolution experiments with high luminosity

External Target Versus Internal Target



The EXL Detector Setup - Concept and Design Goals



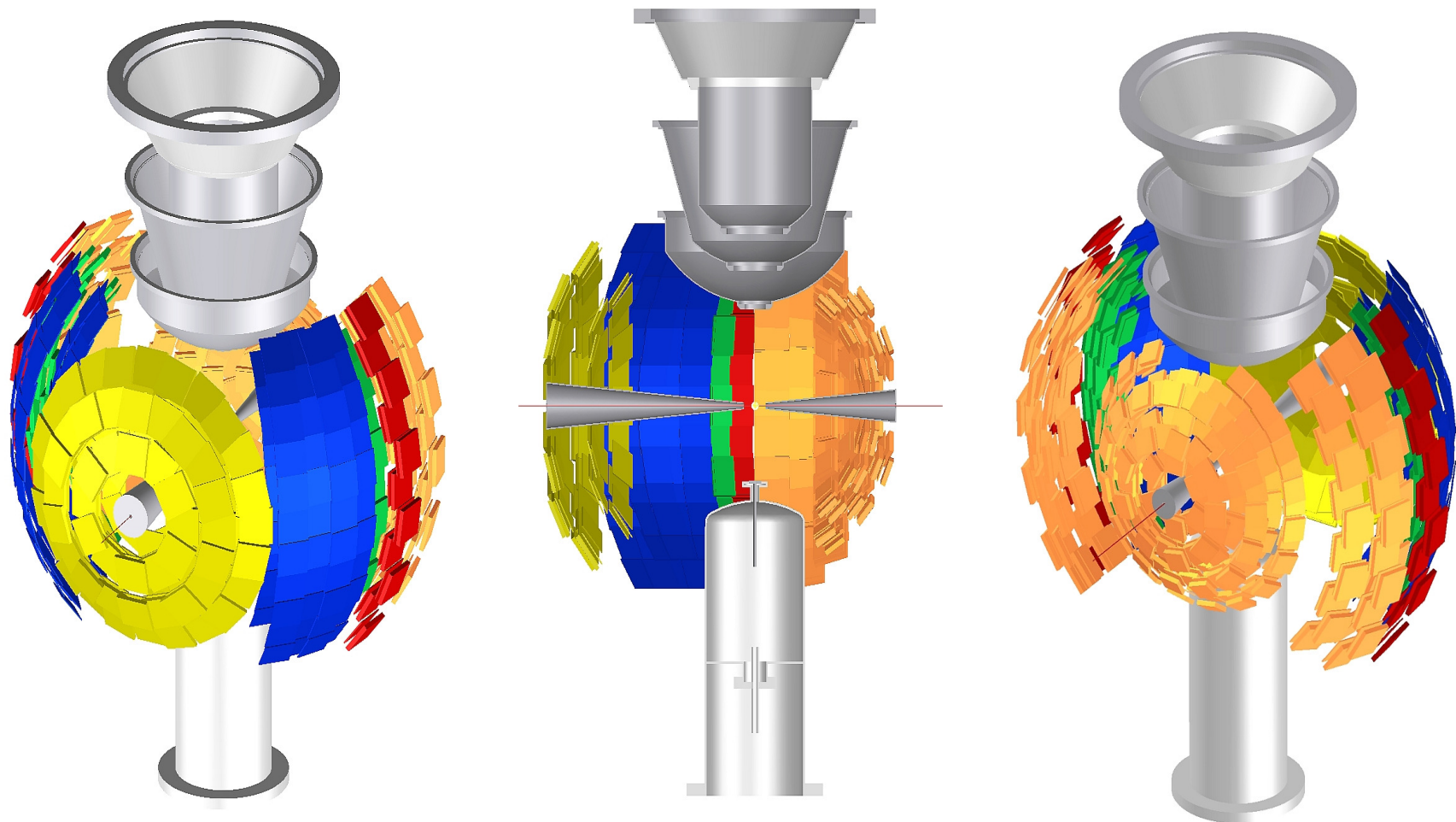
Detection systems for:

- Target recoils and gammas ($p, \alpha, n, \gamma \dots$)
- Forward ejectiles (p, n, γ)
- Beam-like heavy ions

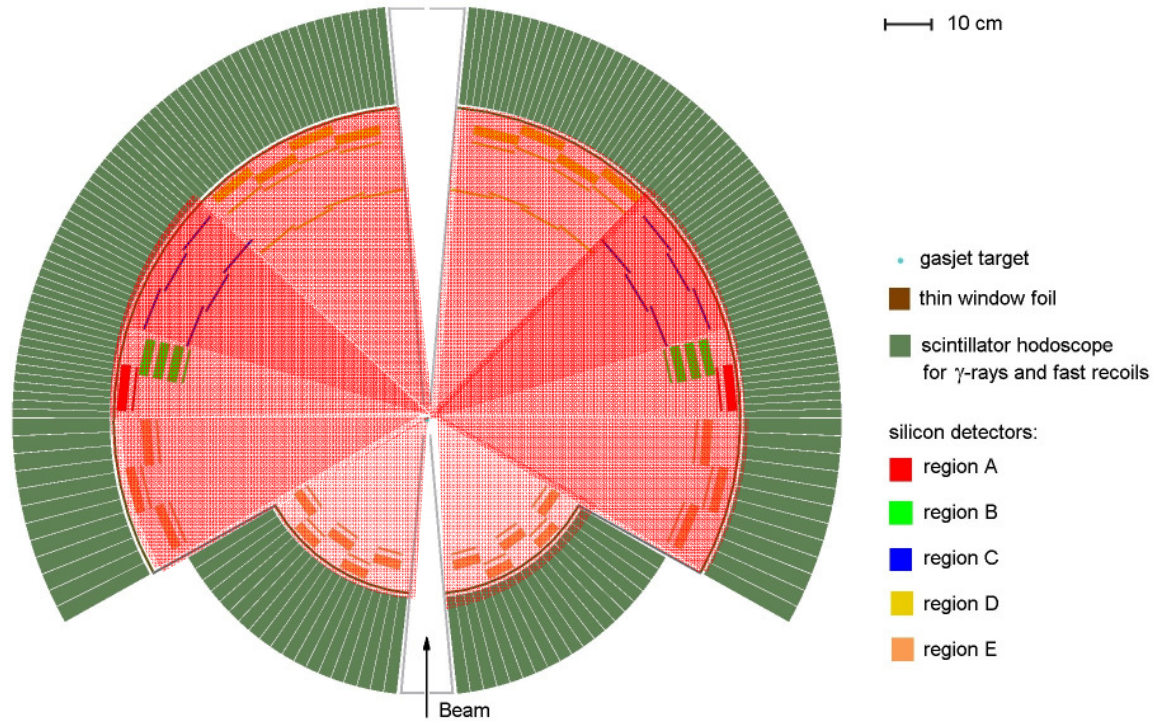
Design goals

- Universality: applicable to a wide class of reactions
- High energy and angular resolution
- Fully exclusive kinematical measurements
- High luminosity ($> 10^{28} \text{ cm}^{-2} \text{ s}^{-1}$)
- Large solid angle acceptance
- UHV compatibility (in part)

The EXL Recoil and Gamma Array



The EXL Recoil and Gamma Array



10 cm

Si DSSD $\Rightarrow \Delta E, x, y$
300 μm thick, spatial resolution better than 500 μm in x and y, $\Delta E = 30 \text{ keV}$ (FWHM)

Thin Si DSSD \Rightarrow tracking
<100 μm thick, spatial resolution better than 100 μm in x and y, $\Delta E = 30 \text{ keV}$ (FWHM)

Si(Li) $\Rightarrow E$
9 mm thick, large area $100 \times 100 \text{ mm}^2$, $\Delta E = 50 \text{ keV}$ (FWHM)

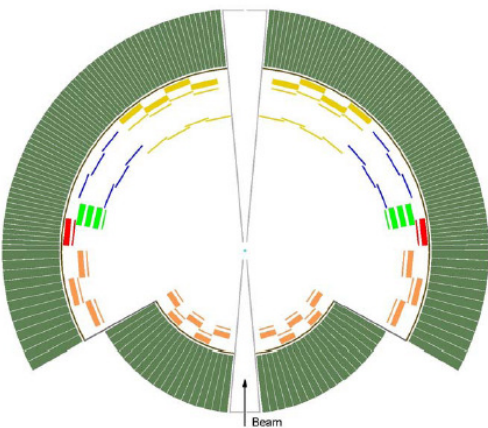
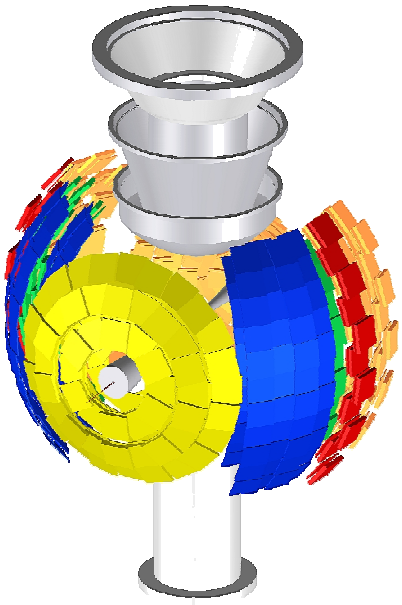
CsI crystals $\Rightarrow E, \gamma$
High efficiency, high resolution, 20 cm thick

classical scattering reactions

Specifications of the Silicon Detectors for EXL

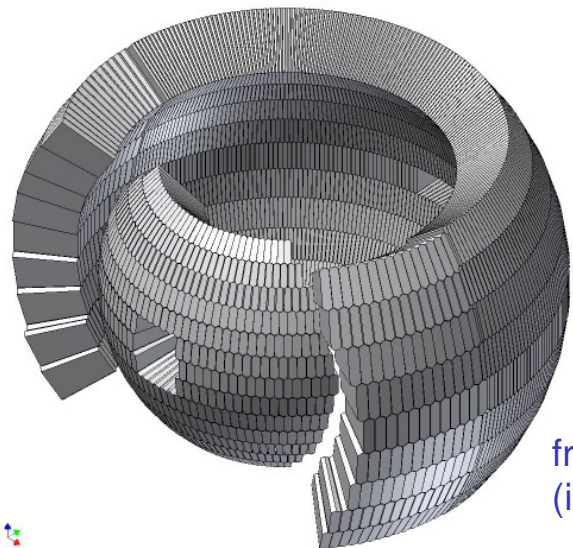
Angular region	Θ_{lab} [deg]	Detector type	Active area [mm ²]	Thickness [mm]	Distance from target [cm]	Pitch [mm]	Number of detectors	Number of channels
A	89 - 80	DSSD Si(Li)	87 x 87 87 x 87	0.3 9	59 60	0.1 -	20 20	34800 180
B	80 - 75	DSSD Si(Li) Si(Li) Si(Li)	50 x 87 50 x 87 50 x 87 50 x 87	0.3 9 9 9	50 52 54 56	0.1 - - -	20 20 20 20	27400 180 180 180
C	75 - 45	DSSD DSSD	87 x 87 87 x 87	0.1 0.3	50 60	0.1 0.1	60 60	104400 34800
D	45 - 10	DSSD DSSD Si(Li)	87 x 87 87 x 87 87 x 87	0.1 0.3 9	49 59 60	0.1 0.1 -	60 80 80	104400 139200 720
E	170 - 120	DSSD Si(Li)	50 x 50 50 x 50	0.3 5	25 26	0.5 -	60 60	6000 240
E'	120 - 91	DSSD Si(Li)	87 x 87 87 x 87	0.3 5	59 60	0.1 -	60 60	104400 540
Total		DSSD Si(Li)					420 280	555400 2220

Specifications of the Silicon Detectors for EXL

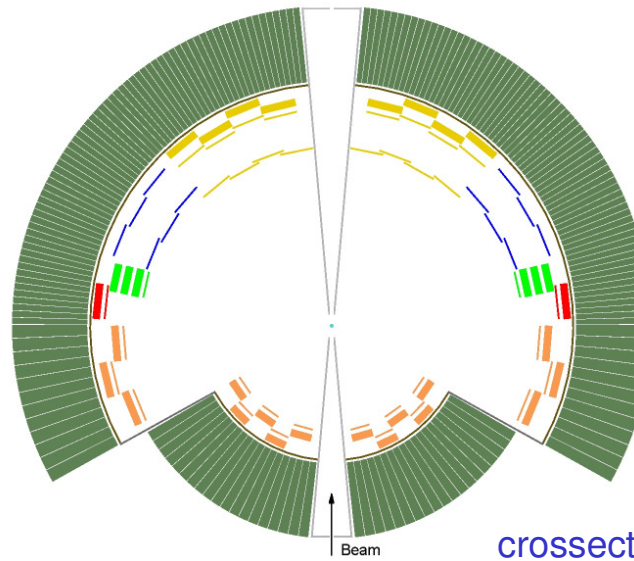


- low threshold ≤ 40 keV
(\Rightarrow constraints on thickness of entrance windows)
- high energy resolution ≤ 20 keV
- pitch size ≥ 0.5 mm
- active area 65×65 mm 2
- large dynamic range: 100 keV to 50 MeV
- readout of energy, time, PSA??
- self triggering
- moderate count rates
- UHV (HV) compatibility (partly)

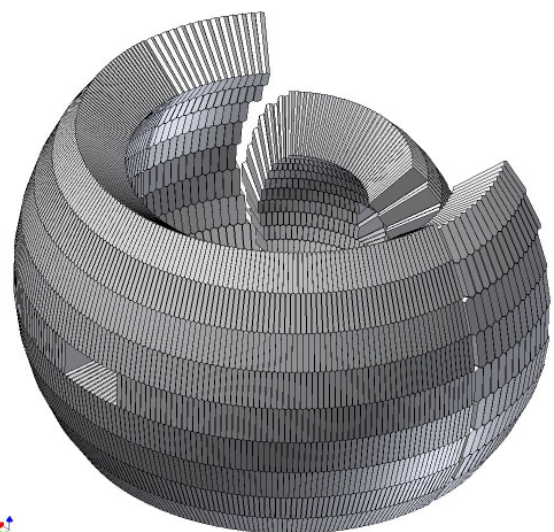
Design Study of the Gamma-Calorimeter



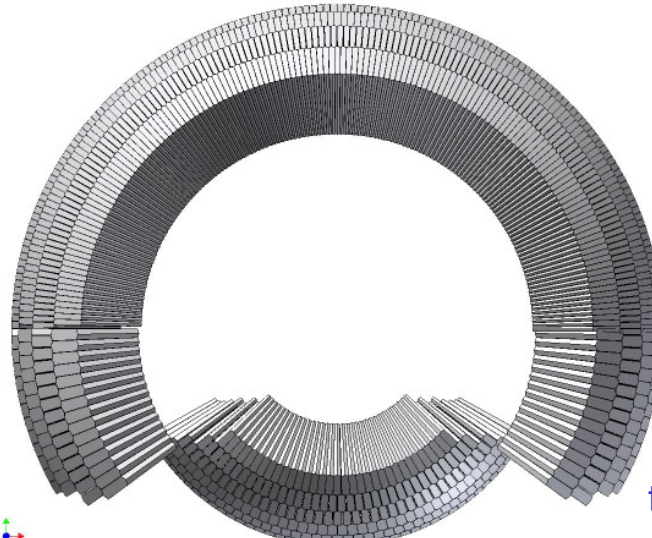
front view
(isometric)



crossection of basic concept



rear view
(isometric)



top view of 3D model

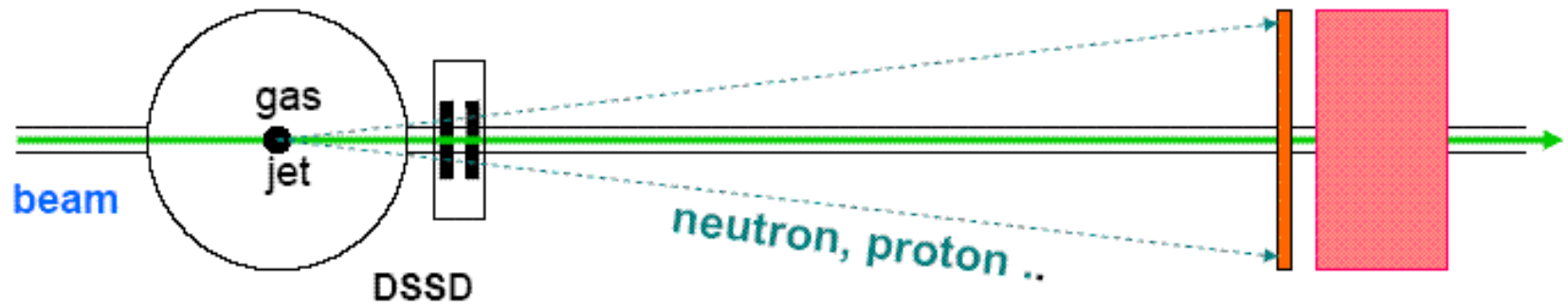
10 cm

- gasjet target
- thin window foil
- scintillator hodoscope for γ -rays and fast recoils
- silicon detectors:
 - region A
 - region B
 - region C
 - region D
 - region E

The EXL Forward Ejectile Detector

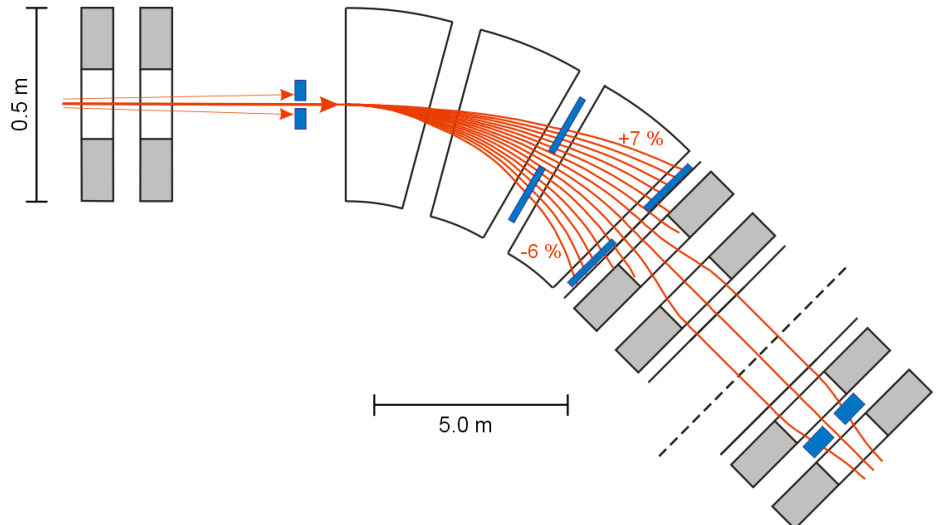
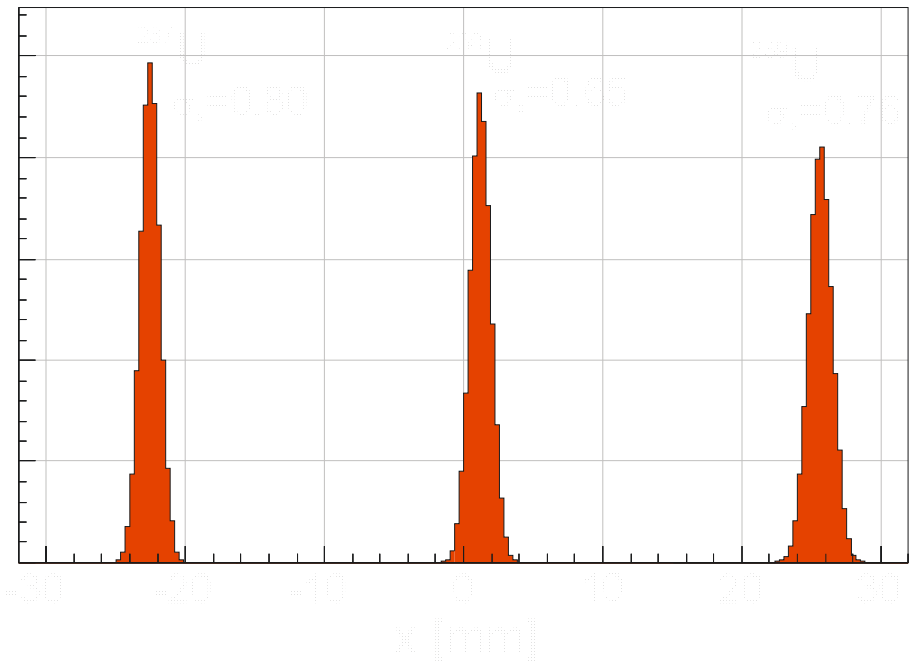
Kinematically complete measurements:

- detection of forward light particles emitted from the projectile (momenta measured)
- excitation energy of projectile residue, momentum (angular) correlations



- High-resolution TOF and position measurements
- Full solid angle (forward focus)
- Calorimeter: scintillator + iron converter (similar to LAND)

The EXL In-Ring Heavy-Ion Spectrometer



- ❖ Ion-optical mode for NESR as fragment spectrometer
- ❖ 3 heavy-ion detector stations:
 - in front of first dipole magnet for 'reaction tagging' (main mode)
 - inserted into dipole section for 'tracking' of fragments
 - inserted into quadrupole section for 'imaging' properties of magnetic Spectrometer (limited acceptance)

Predicted Luminosities

Target: 10^{14} H atoms cm $^{-2}$; beam losses included

740 A.MeV 100 A.MeV

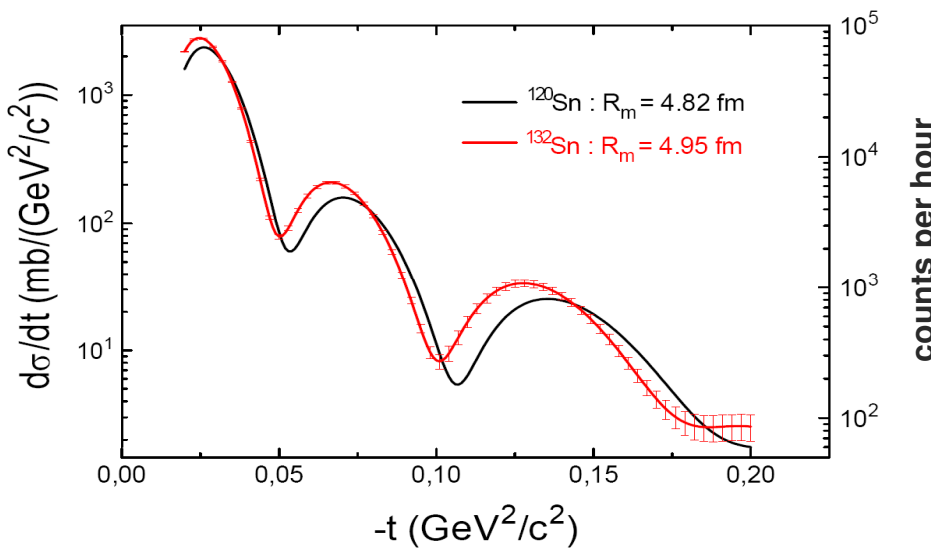
Nucleus	production rate at S-FRS target [1/s]	Lifetime including losses in NESR [s]	Luminosity [cm $^{-2}$ s $^{-1}$]	Luminosity [cm $^{-2}$ s $^{-1}$]
^{11}Be	2×10^9	36	$> 10^{28}$	$> 10^{28}$
^{46}Ar	6×10^8	20	$> 10^{28}$	$> 10^{28}$
^{52}Ca	4×10^5	12	2×10^{26}	4×10^{25}
^{55}Ni	8×10^7	0.5	6×10^{26}	5×10^{25}
^{56}Ni	1×10^9	3800	$> 10^{28}$	$> 10^{28}$
^{72}Ni	9×10^6	4.1	2×10^{27}	3×10^{26}
^{104}Sn	1×10^6	51	3×10^{27}	6×10^{26}
^{132}Sn	1×10^8	93	$> 10^{28}$	$> 10^{28}$
^{134}Sn	8×10^5	2.7	3×10^{25}	5×10^{24}
^{187}Pb	1×10^7	34	$> 10^{28}$	3×10^{27}

Options to be explored: Deceleration, Multi-charge state operation (*increase luminosity*) ?

Expected Performance

Elastic proton scattering ^{132}Sn (Matter Distribution)

Skin and halos in heavy neutron-rich nuclei

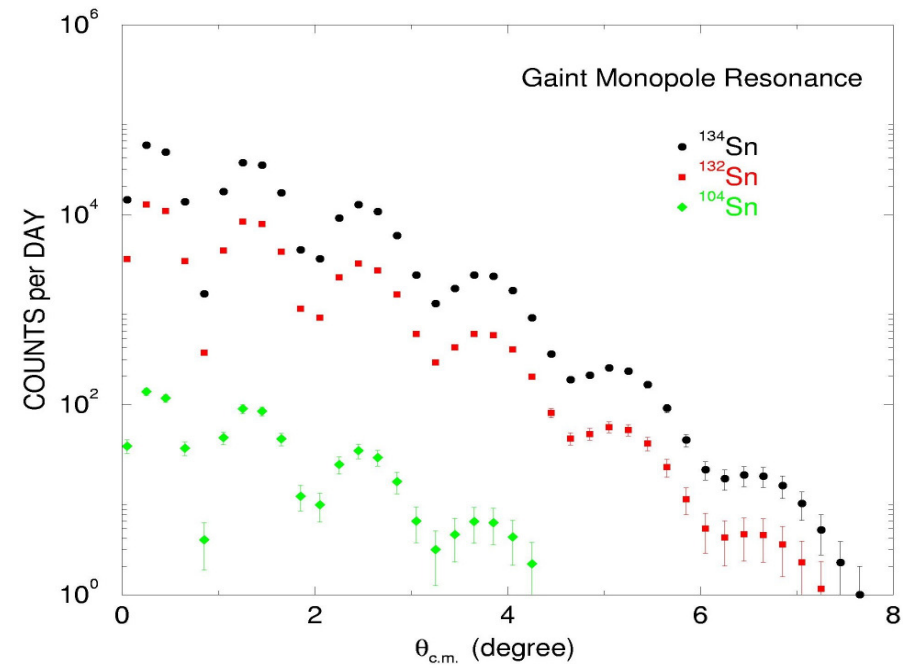


High sensitivity of the method
(simulation of experimental conditions
as expected at the NESR with a
luminosity of $10^{28} \text{ cm}^{-2} \text{ s}^{-1}$)

at present ESR: needs 500 days !!!

Inelastic alpha scattering on Sn isotopes (Giant Monopole Resonance)

Collective modes in asymmetric
nuclei, nuclear matter compressibility



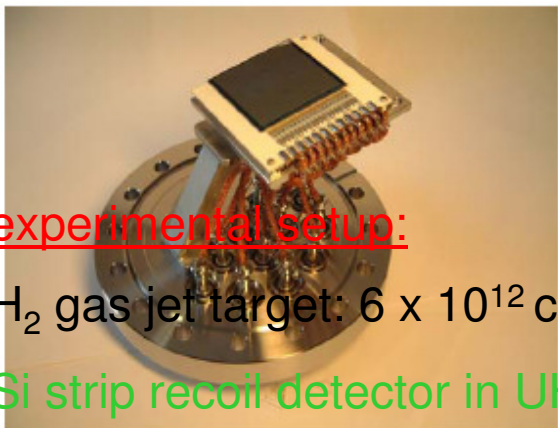
at present ESR: needs 10000 days !!!

R&D and Feasibility Studies for EXL:

a) First Feasibility Demonstration for EXL performed at the ESR

experimental conditions:

- ^{136}Xe beam, $E = 350 \text{ MeV/u}$
- 10^9 circulating ions in ring $\Rightarrow L \approx 6 \cdot 10^{27} \text{ cm}^{-2} \text{ sec}^{-1}$



experimental setup:

H_2 gas jet target: $6 \times 10^{12} \text{ cm}^{-2}$

Si strip recoil detector in UHV

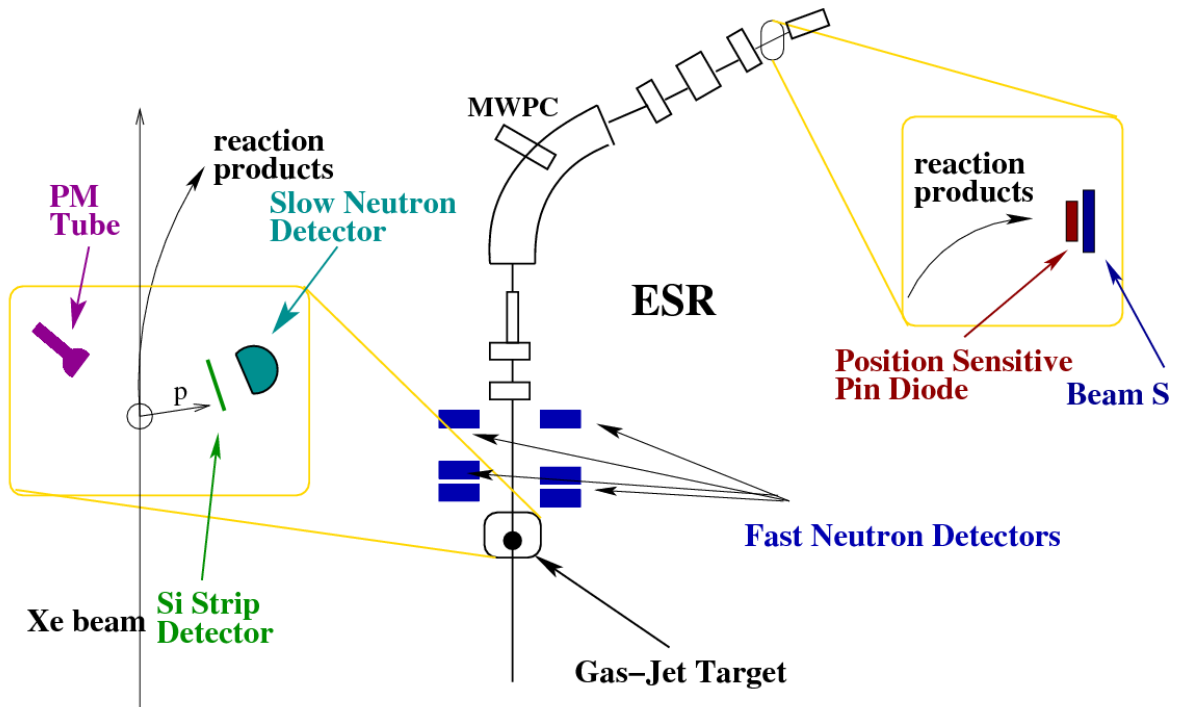
detector for slow neutrons

detectors for

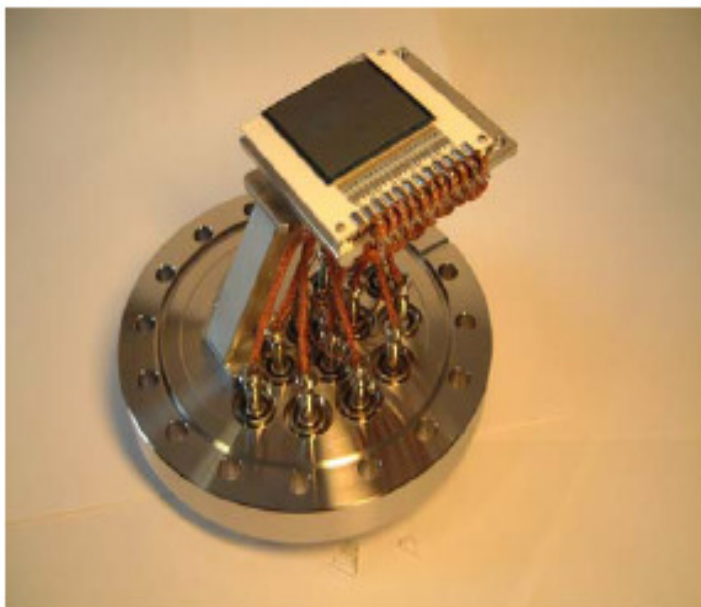
fast neutrons and protons

forward heavy ion detection

3 different luminosity monitors



Si-Strip Detector for Applications under UHV Conditions



- design:

- active area: $40 \times 40 \text{ mm}^2$
- thickness: 1 mm
- 40 strips (pitch: 1mm) connected for readout in groups of 8
- bakeable to $250^\circ \text{ Celsius}$
- cables: home made

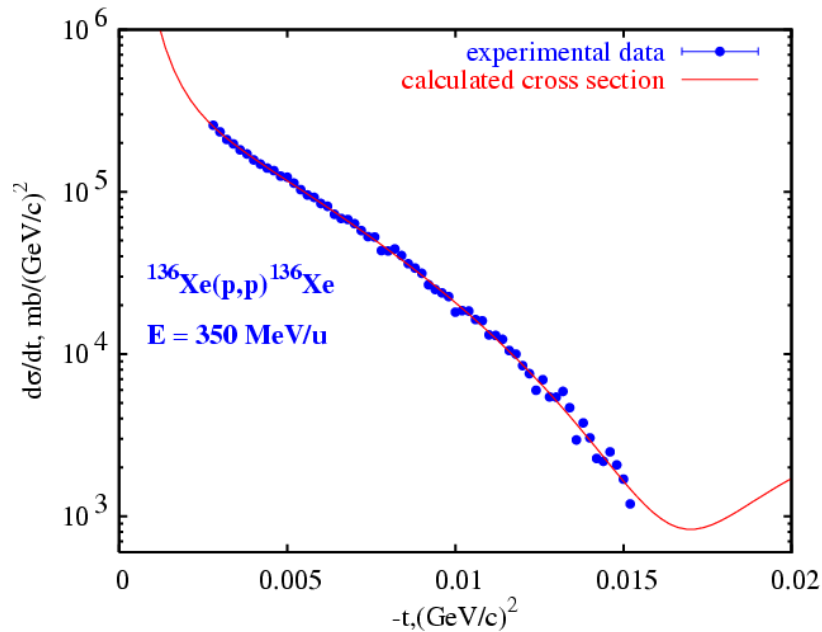
- performance:

- energy resolution 35 keV FWHM
- low outgassing rate

Selected Results

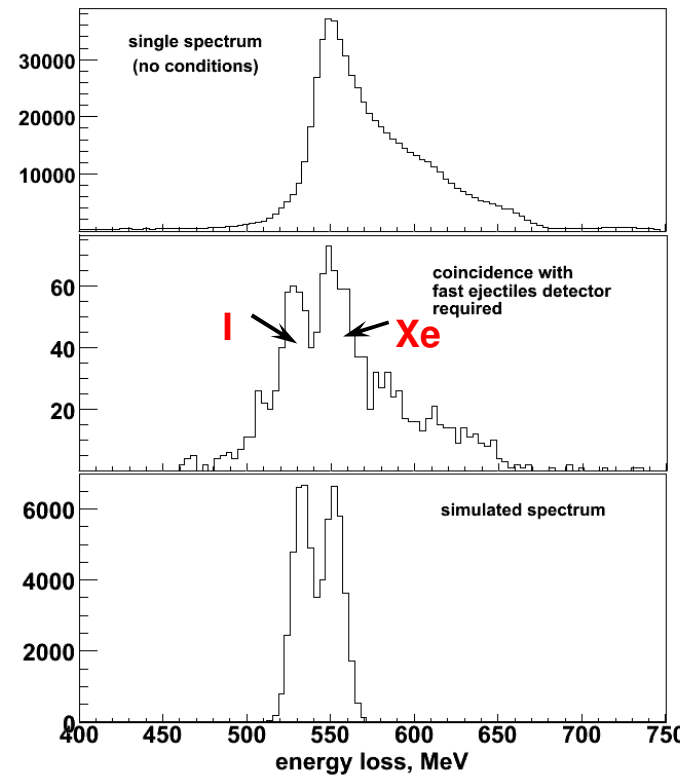
H. Moeini and S. Ilieva et al., NIM A634 (2011)77

Recoil Detector in UHV:
Differential $^{136}\text{Xe}(p,p)$ cross section

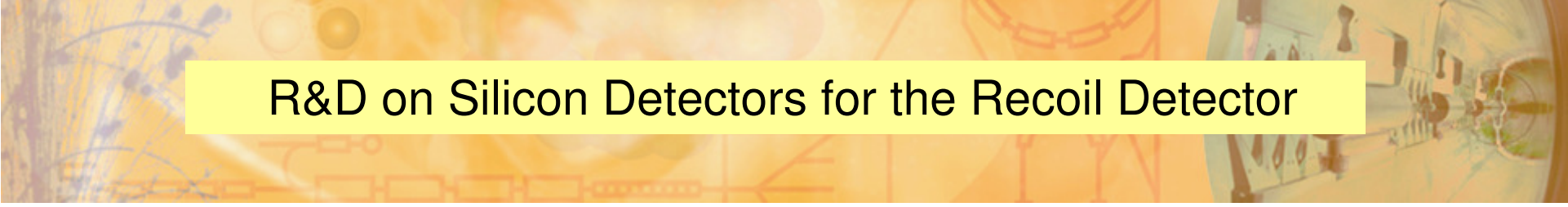


data are consistent with
nuclear matter radius: $R_m = 4.89 (10) \text{ fm}$
(expected from data on the charge radius)

In-Ring Detectors:
Identification of reaction channels



identified reaction channels :
 $^{136}\text{Xe}(p, pn)^{135}\text{Xe}$
 $^{136}\text{Xe}(p, 2pxn)^{132,133}\text{I}$



R&D on Silicon Detectors for the Recoil Detector

Aim: determine spectroscopic properties: ΔE , $\Delta(dE)$, efficiency, PSD
resolution of total energy reconstruction
UHV capability

Detectors: 1st series of DSSDs from PTI St. Petersburg
(8 sensors delivered April 2008/ September 2009)
2nd series of DSSD's with larger size (65 x 65 mm²)
(5 sensors delivered January 2010)

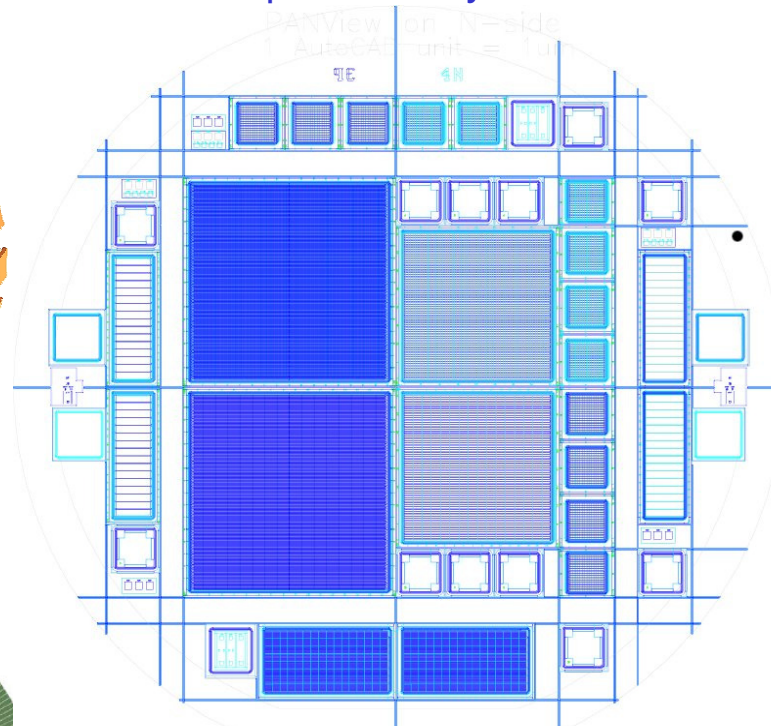
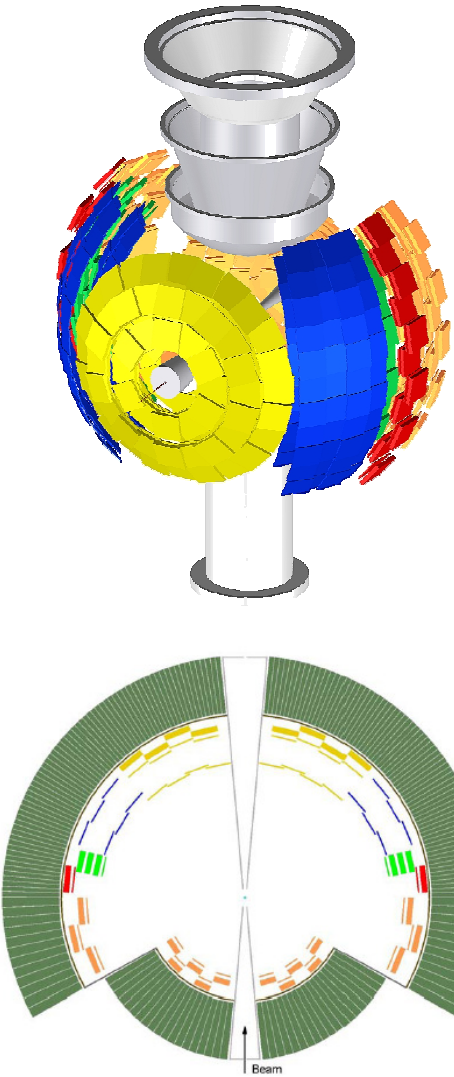
Tests:

2008/2009: GSI:	α sources
2008: Edinburgh:	α sources
April 2009: KVI Groningen:	protons of 50 MeV
July 2009: TU München:	α particles $E < 30$ MeV
September 2009: GSI:	protons of 100 and 150 MeV
April 2010: KVI Groningen:	protons of 135 MeV

Status and Perspectives of R&D

Si - Detectors: DSSD`s

sensors provided by PTI St. Petersburg (V. Eremin et al.)

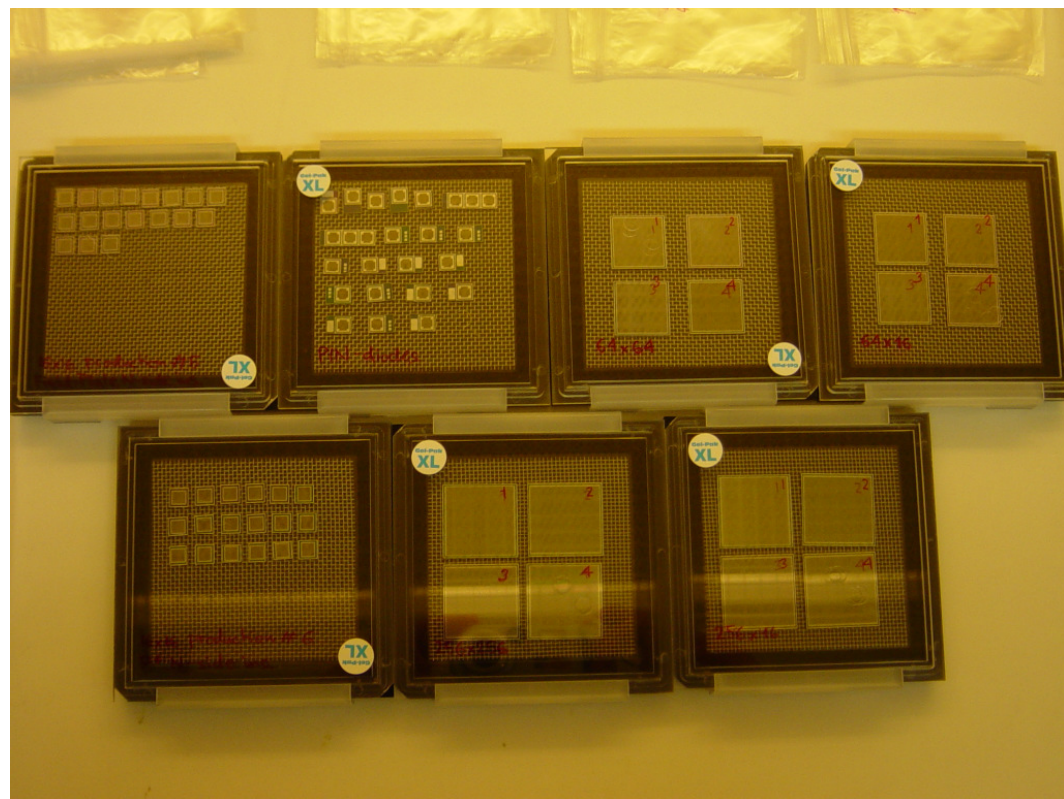


⇒ various test structures for R&D:

- a) $21 \times 21 \text{ mm}^2$, strip pitch $300 \mu\text{m}$ on both sides
- b) $27 \times 27 \text{ mm}^2$, strip pitch $100 \mu\text{m}$ on both sides
- c) $27 \times 27 \text{ mm}^2$, strip pitch $100 \mu\text{m}$, and 2.5 mm on the other side
- d) $21 \times 21 \text{ mm}^2$, strip pitch $300 \mu\text{m}$, and 1.25 mm on the other side
- e) many smaller-size test structures

DSSD Chips

Production – PTI St. Petersburg (Russia) Si wafer (300 μ m thick, 4")

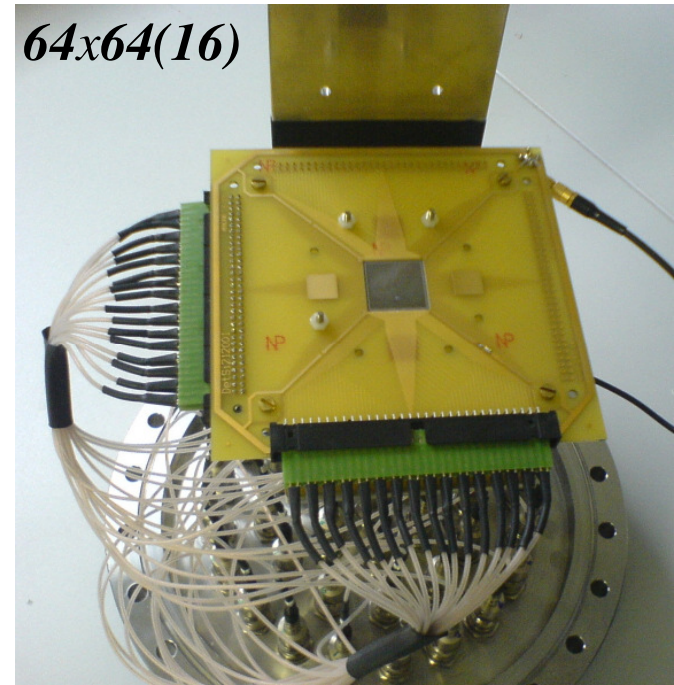
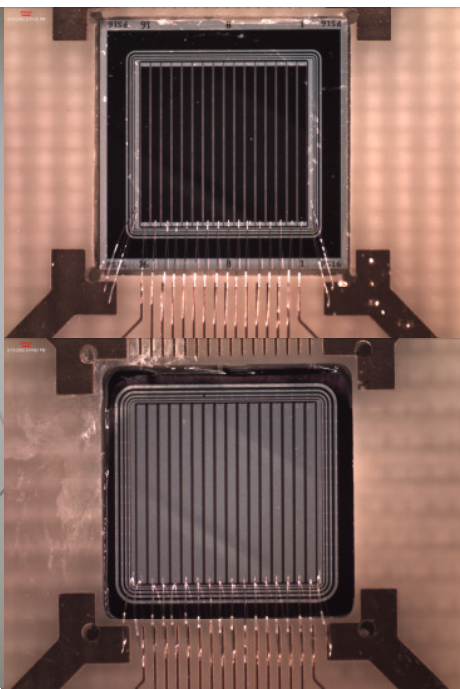
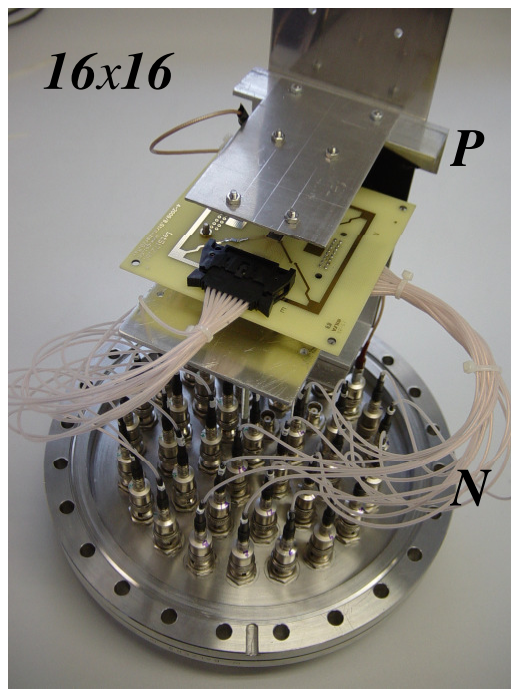


Available DSSDs

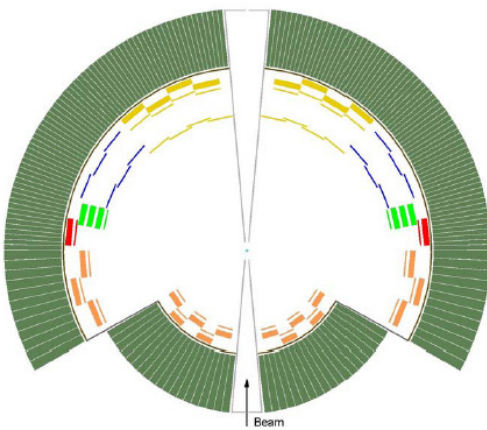
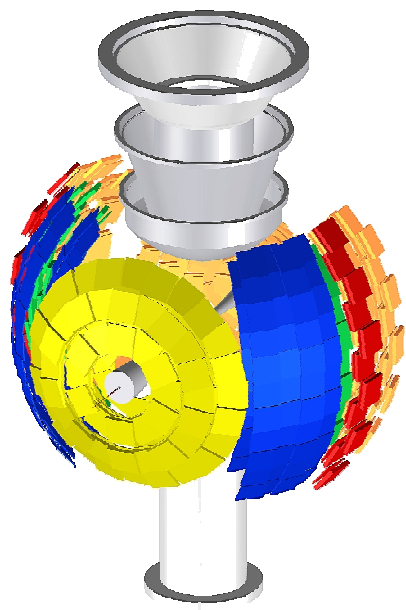
pitch	P+	N+	No
300 μ m	16 x 16 (FP):		20
300 μ m	16 x 16 (P ⁺):		20
300 μ m	64 x 16:		4
300 μ m	64 x 64:		4
100 μ m	256 x 16:		4
100 μ m	256 x 256:		4
	PIN:		30

Detector Construction at GSI

- Construction of prototype DSSDs at GSI: **16x16 (4)**, **64x64 (4) + 64x16 (4)**
- Both types use FR-4 PCB with epoxy-glued DSSD chips
- Wedge bonded



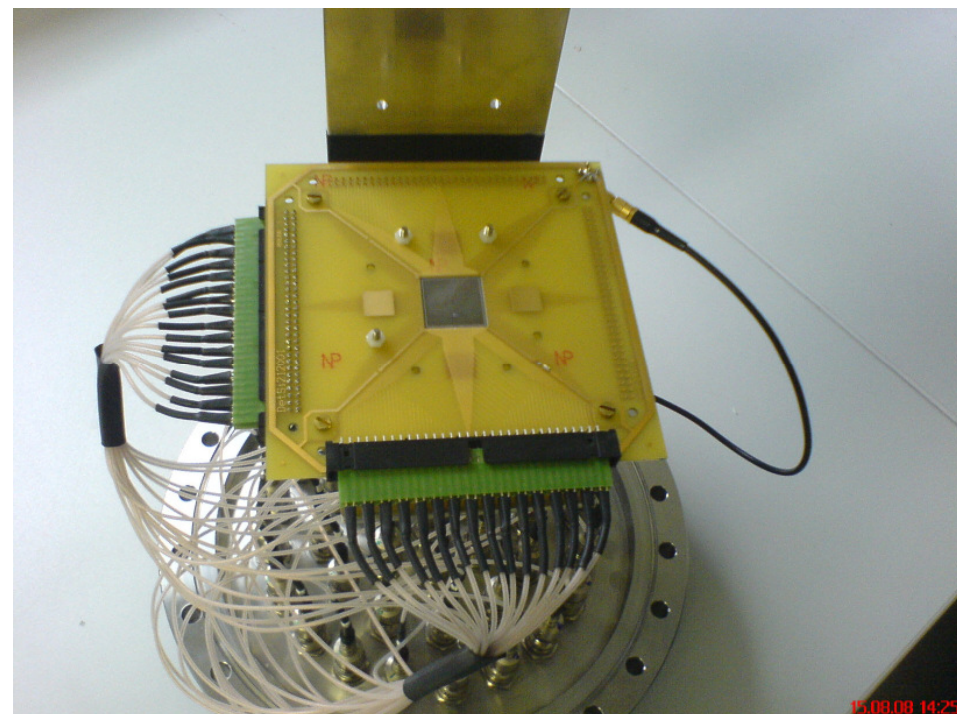
Status and Perspectives of R&D



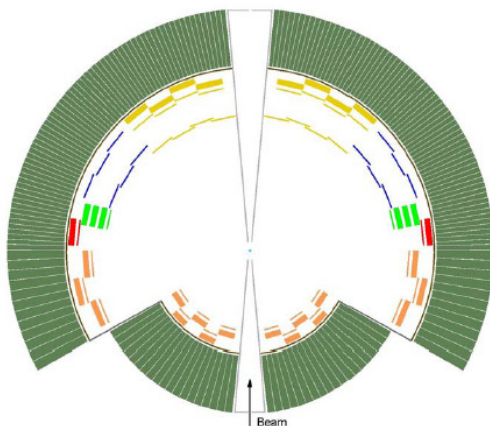
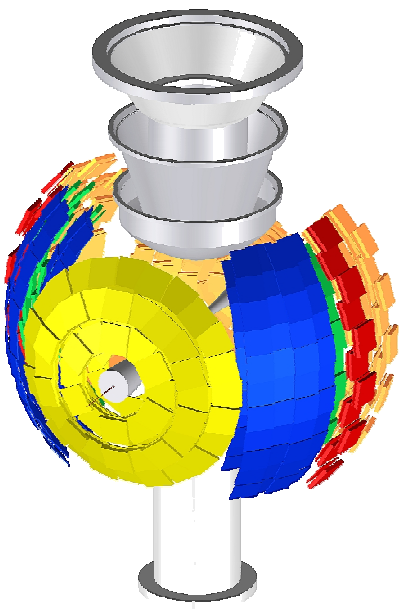
Si - Detectors: DSSD`s

sensors provided by PTI St. Petersburg (V. Eremin et al.)

setup of working detectors (PCB-board, bonding, readout) at GSI
⇒ 9 detectors: 16X16, 64X16, 64X64 strips, d=300 µm



Status and Perspectives of R&D

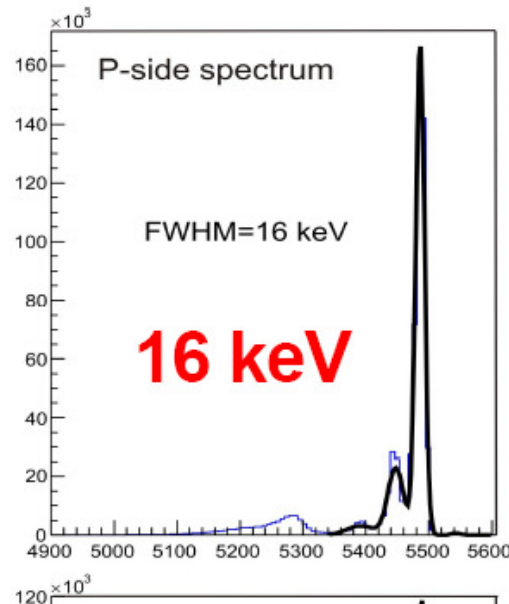


Si - Detectors: DSSD's

sensors provided by PTI St. Petersburg (V. Eremin et al.)

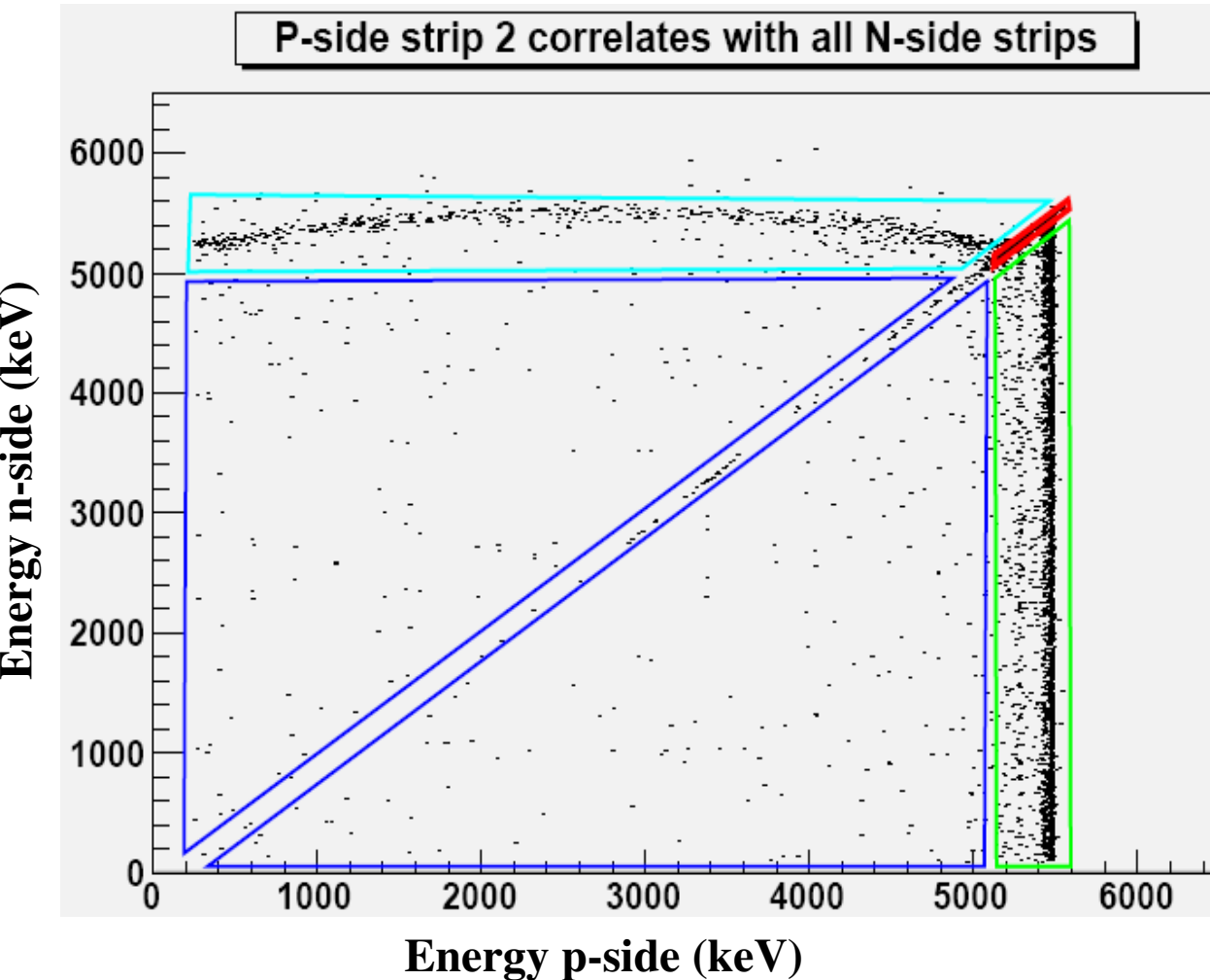
setup of working detectors (PCB-board, bonding, readout) at GSI
⇒ 9 detectors: 16X16, 64X16, 64X64 strips, d=300 µm

detector tests with α-source performed at GSI and Edinburgh
⇒ up to 128 channels read out, up to 99% working strips, $\Delta E=16\text{keV}$



front-rear correlation analysis
⇒ energy resolution and efficiency for p-side and n-side injection
⇒ results to be used as input for design of next generation detectors

Front-Rear Side Correlation Analysis



Event type

P - N

Strip – Strip **76,8 %**

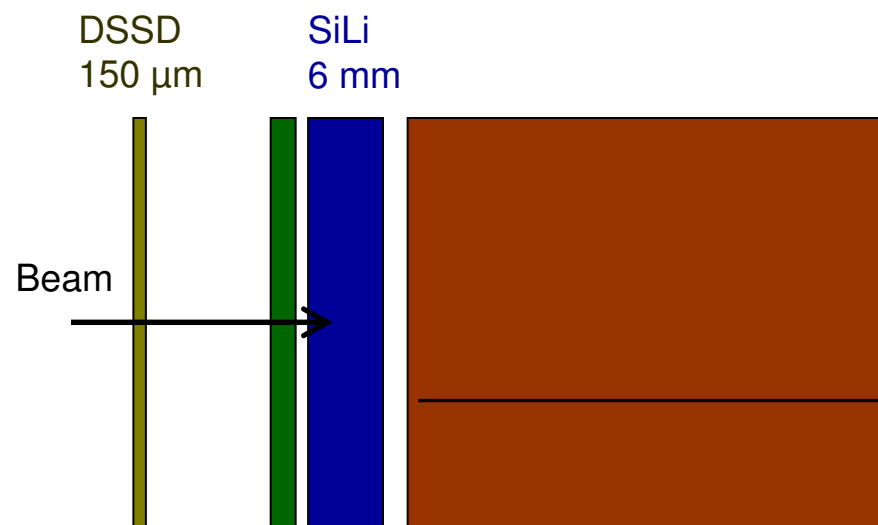
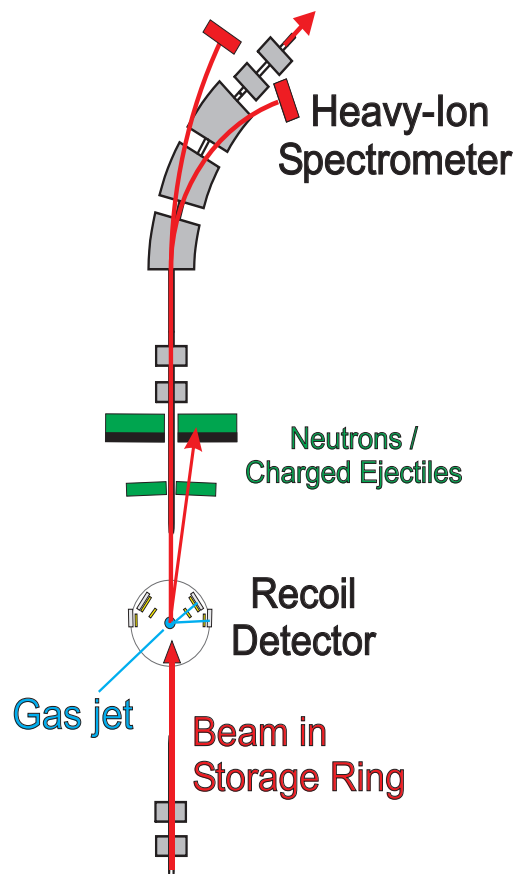
Strip – Interstrip **18,2%**

Interstrip – Strip **4,1%**

Interstrip – Interstrip **0,9%**

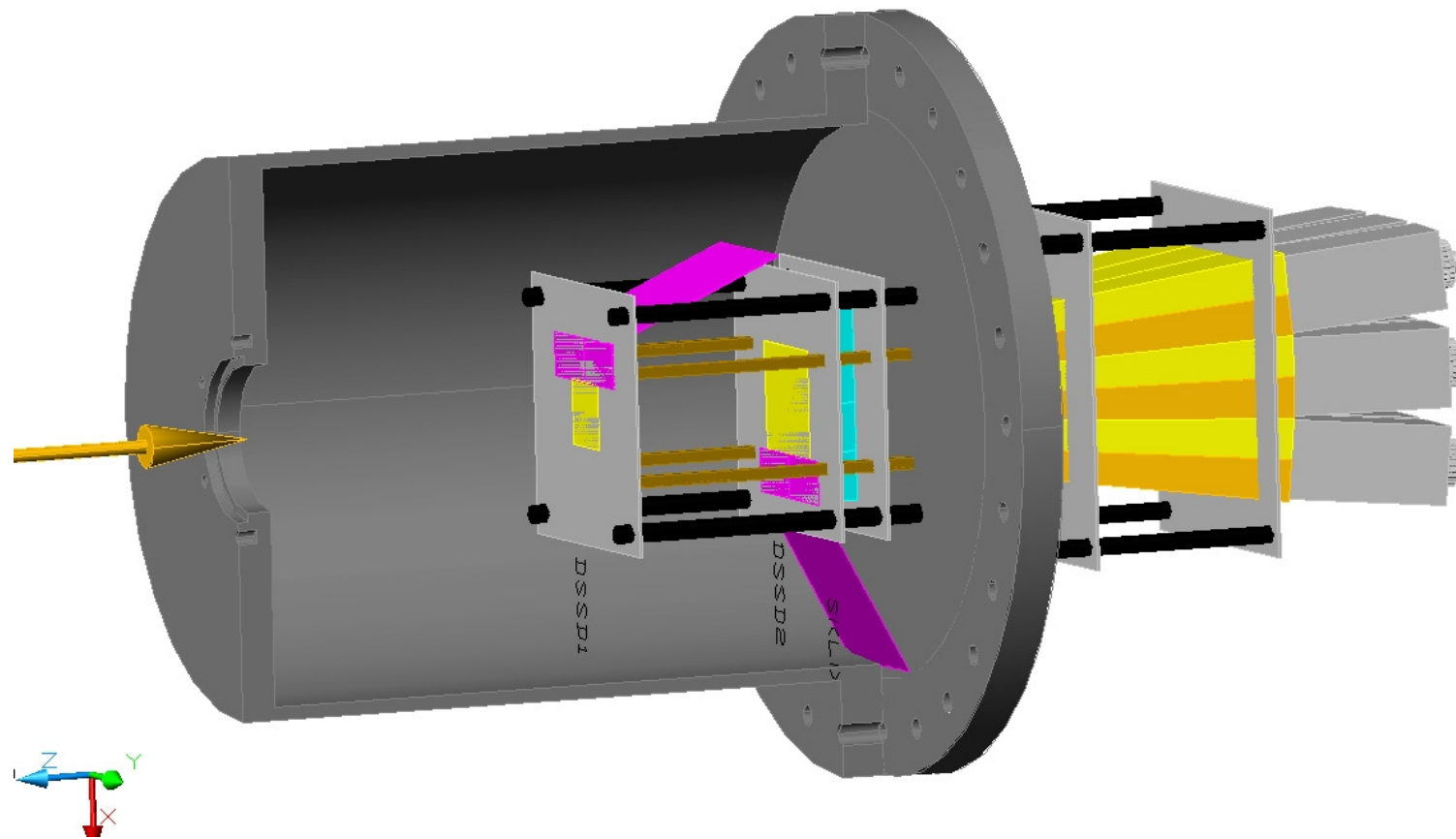
Probabilities
correspond to
pitch structure !

In-Beam Tests with the EXL Demonstrator

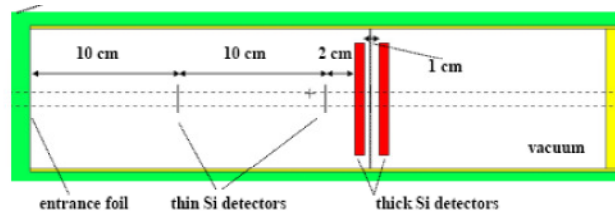
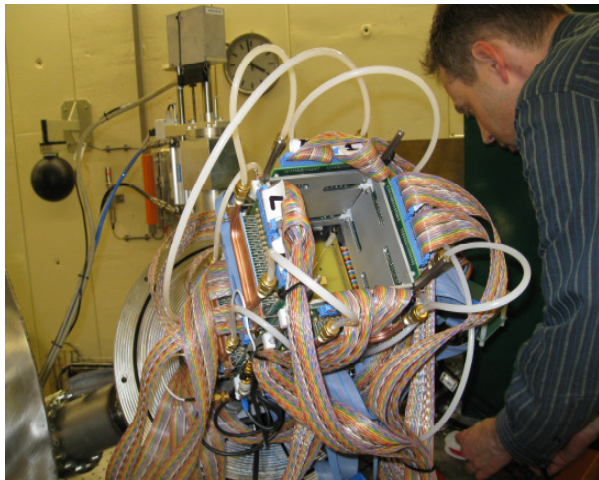


First DSSD – $3 \times 3 \text{ cm}^2$, 64 x 64 strips, pitch 300 µm
Second DSSD – $3 \times 3 \text{ cm}^2$, 64 x 64 strips, pitch 300 µm
SiLi – $9 \times 5 \text{ cm}^2$, 4 x 2 pads
CsI – 3×3 crystals with the individual readout

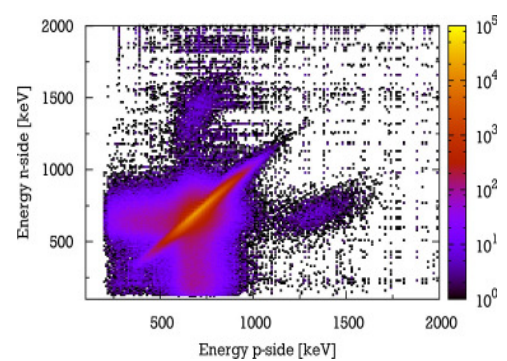
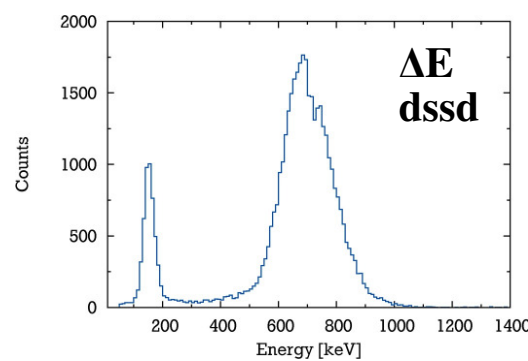
The EXL Demonstrator



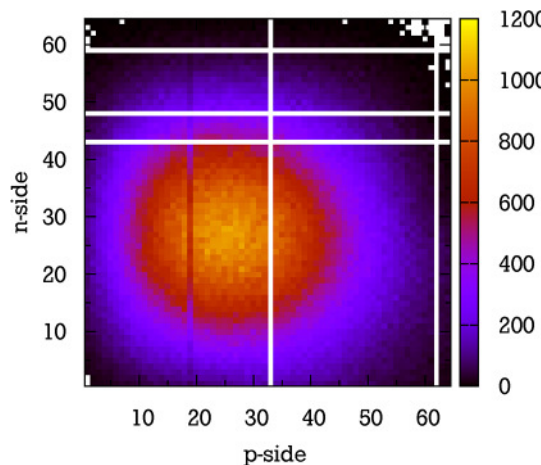
In-Beam Tests at KVI Groningen with 50 MeV Protons



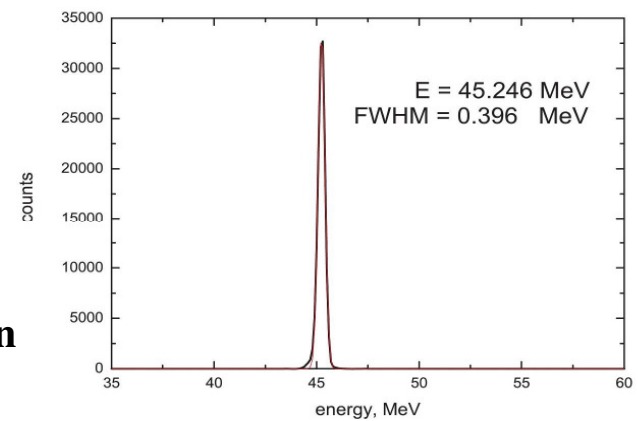
set-up



N/P



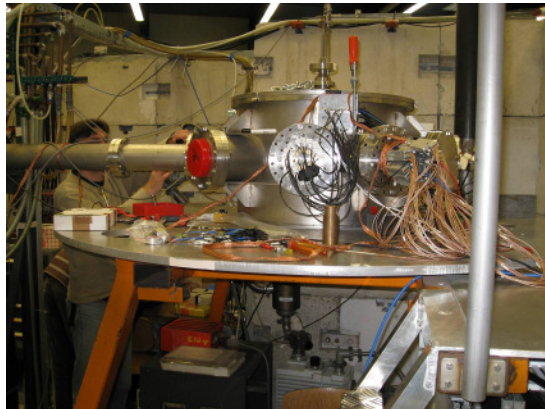
Beam
profile



Total energy
reconstruction

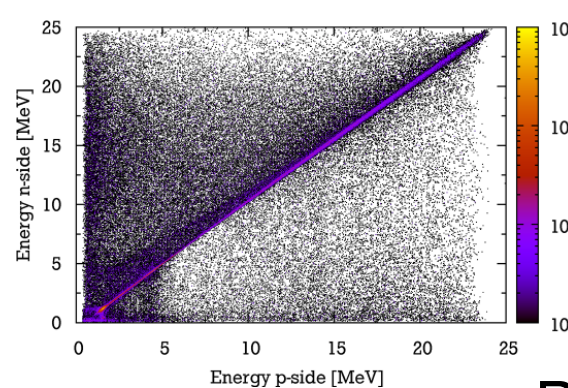
Pulse-Shape Discrimination with DSSD's

test with p, d, ${}^4\text{He}$ from
 ${}^{12}\text{C} + {}^{12}\text{C}$ @ 70 MeV
TU Munich

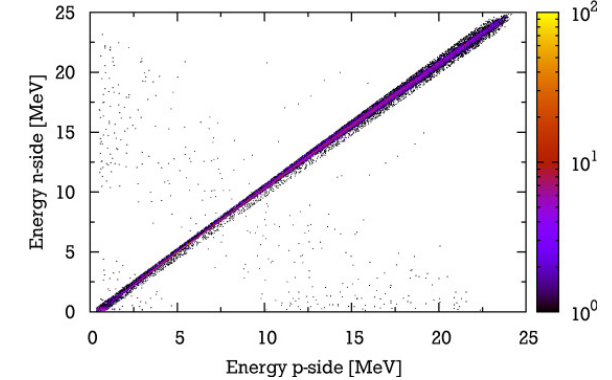


M. von Schmid et al.
NIM A629 (2011)197

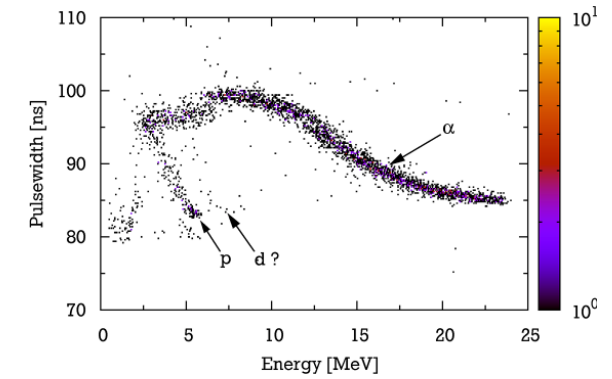
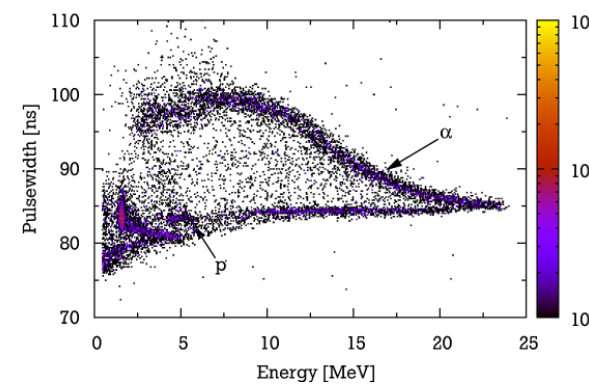
Strip & Interstrip



Strip (stopped α 's)



P/N



PSD

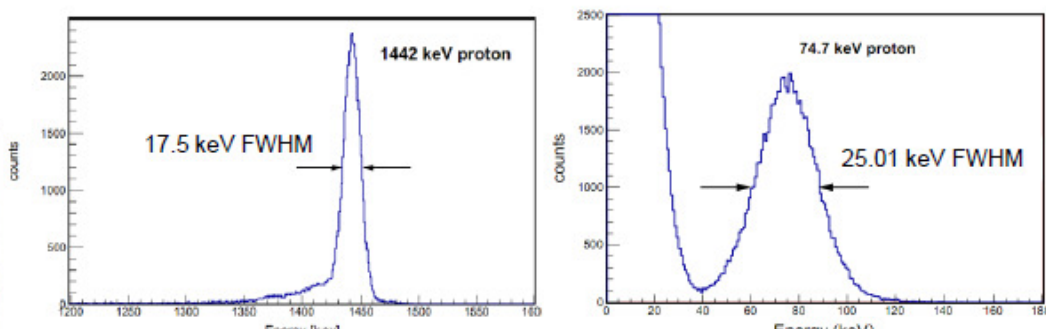
DSSD strip-strip events show PSD comparable with single PIN diodes

Response to very low energy recoil particles

Y. Ke et al.
to be published

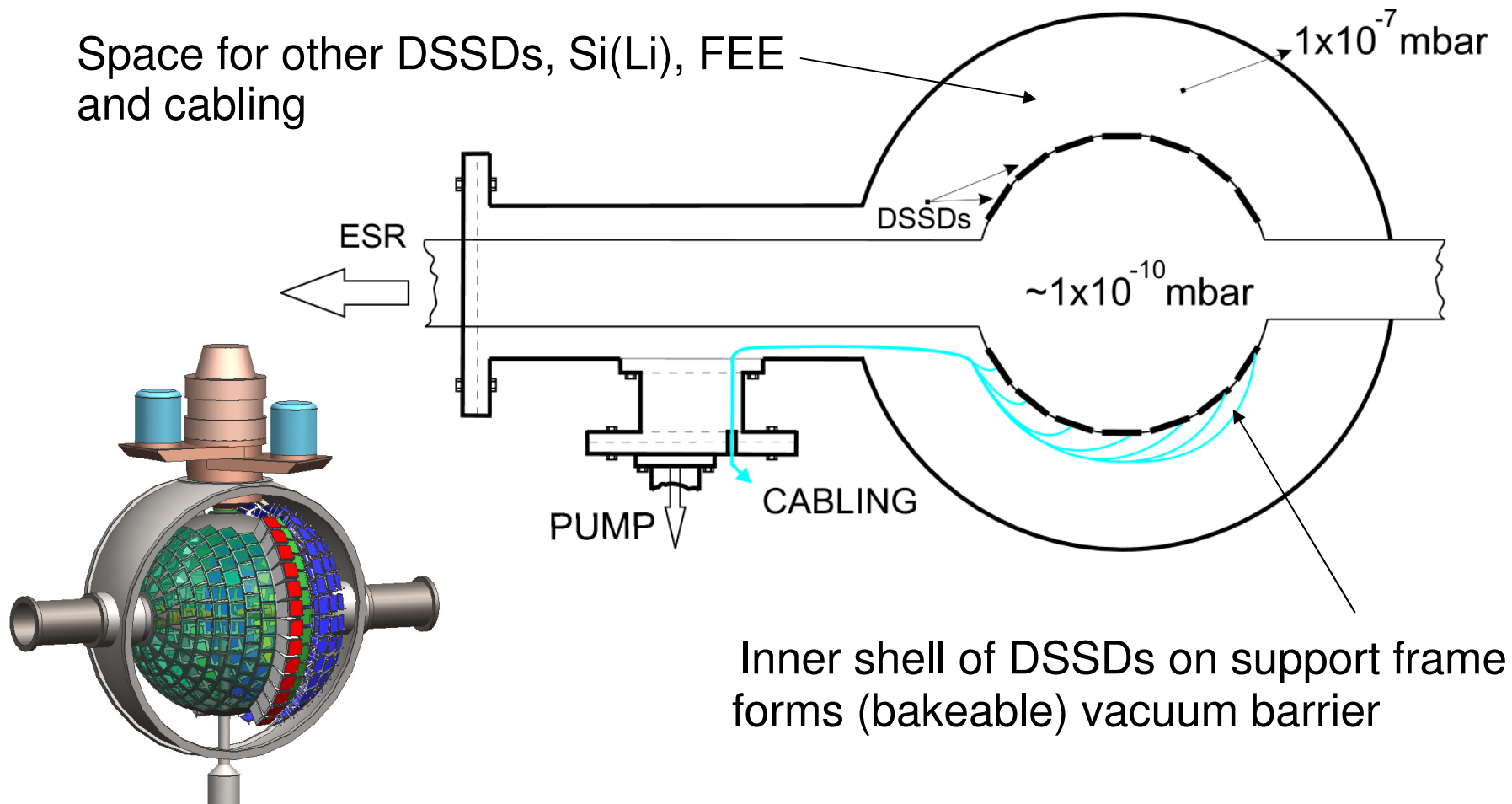


- 1503keV protons scattered from C target ($37\mu\text{g}/\text{cm}^2$)
- Spectrum shows strip #11 (p side)
- 818keV H_2 scattered from C target ($37\mu\text{g}/\text{cm}^2$),
 $\sim 3.5\mu\text{m}$ Mylar degrader in front of DSSD
- Spectrum shows strip #11 (p side)



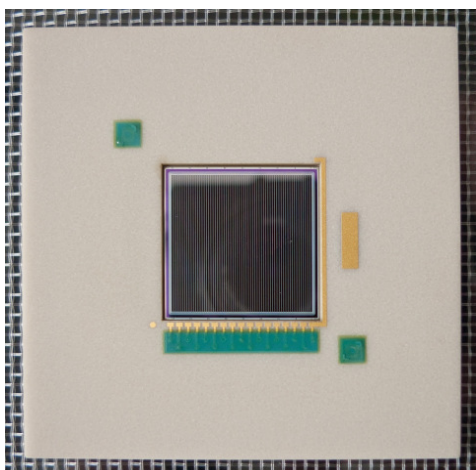
UHV Capability of the EXL Silicon Ball: Concept: using DSSD's as high vacuum barrier

- Differential pumping proposed to separate NESR vacuum from EXL instrumentation (cabling, FEE, other detectors)

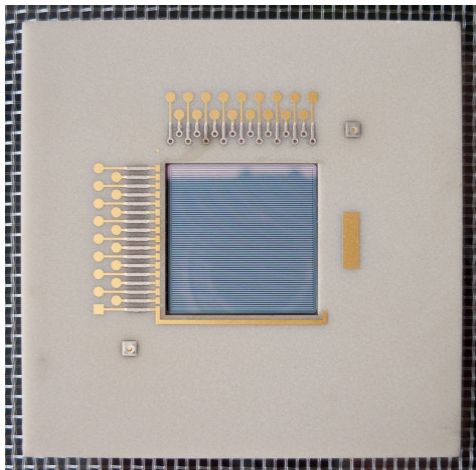


UHV-Barrier DSSD Prototype Design

P-side: in UHV



N-side



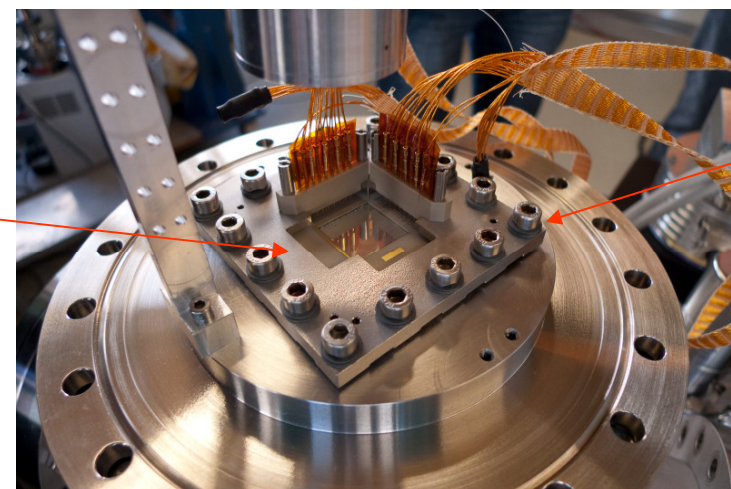
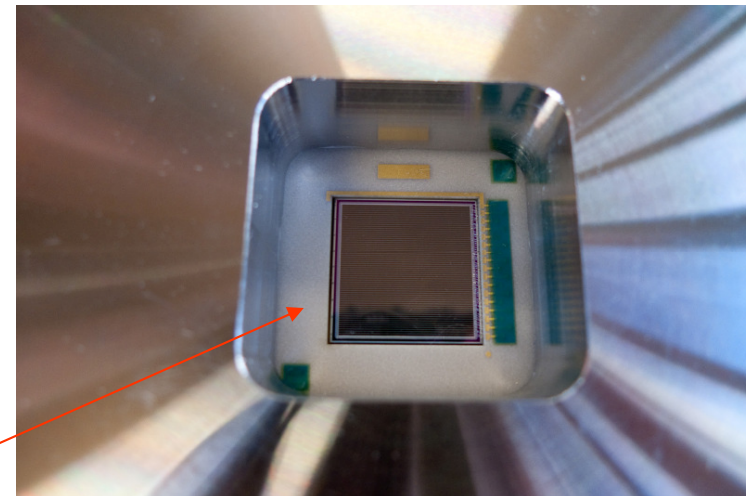
LUST
HYBRID-TECHNIK

21 x 21 mm²
DSSD with
64x64(16) strips
mounted into
AlN PCB of
60 x 60 mm²

P-side towards
UHV

N-side and
spring-pin
connectors at
auxiliary
vacuum

IDI
INTERCONNECT DEVICES, INC.

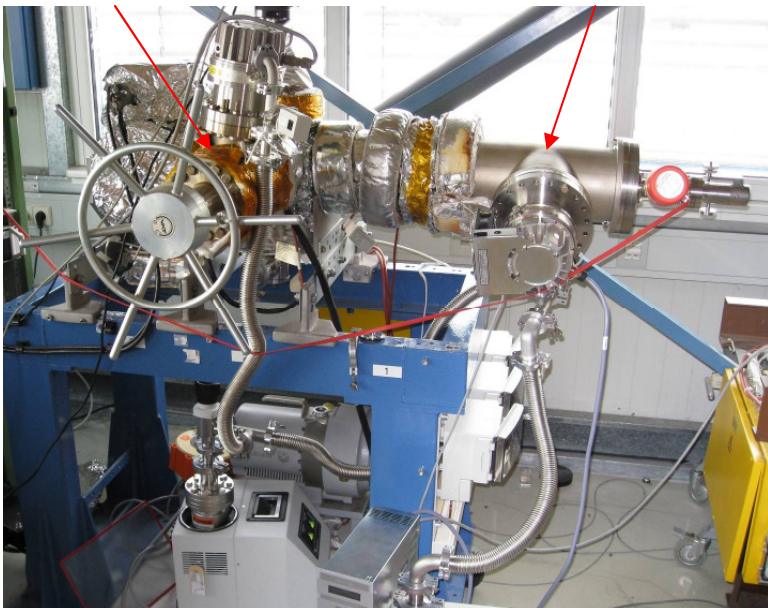


Cup springs

Differential Vacuum Test

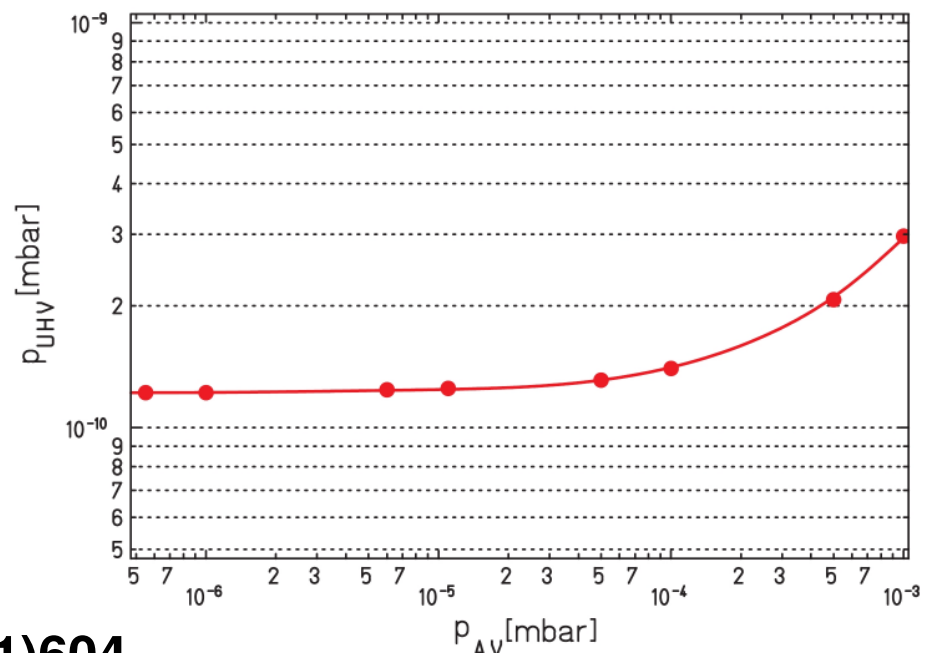
- Differential vacuum test using **real DSSD** as a vacuum barrier
 - ◆ **6 orders of magnitude difference between low and UH vacuum in wide pressure region**
- Vacuum of **$1.2 * 10^{-10}$ mbar** reached – pumping limit of the station

UHV part



Low vacuum part

Vacuum separation

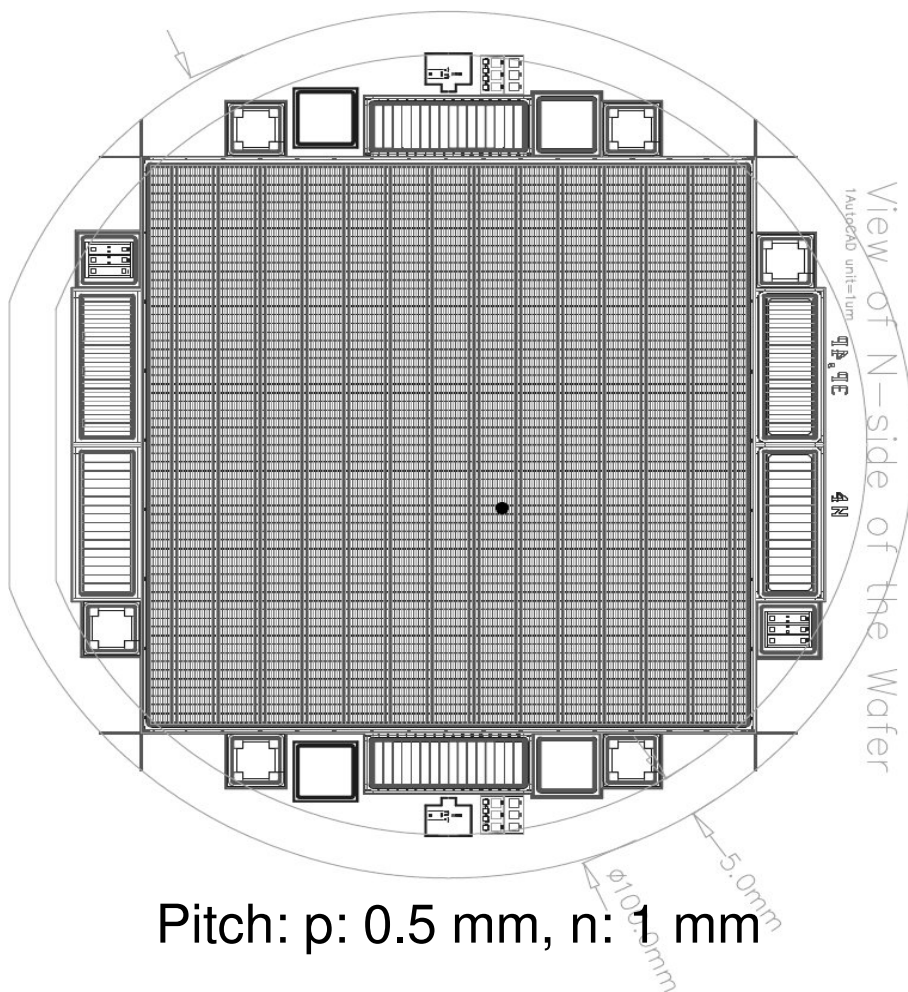


B. Streicher et al., NIM A654 (2011)604

Pespectives:

2nd Series of DSSD's from PTI St. Petersburg: 64 X 64 mm²

65 x 65 mm²



Specification:

Single-crystal silicon: 7 - 20 kOhm×cm

Diode structure: p+ (strips) – i - n+ (strips), orthogonal, n+ - strip insulation, p+ implant

Diode area: 65 x 65 mm²

Diode topology: Strips on p+ side, 128 Strips on n+ side, 64

Diode thickness: 300 µm

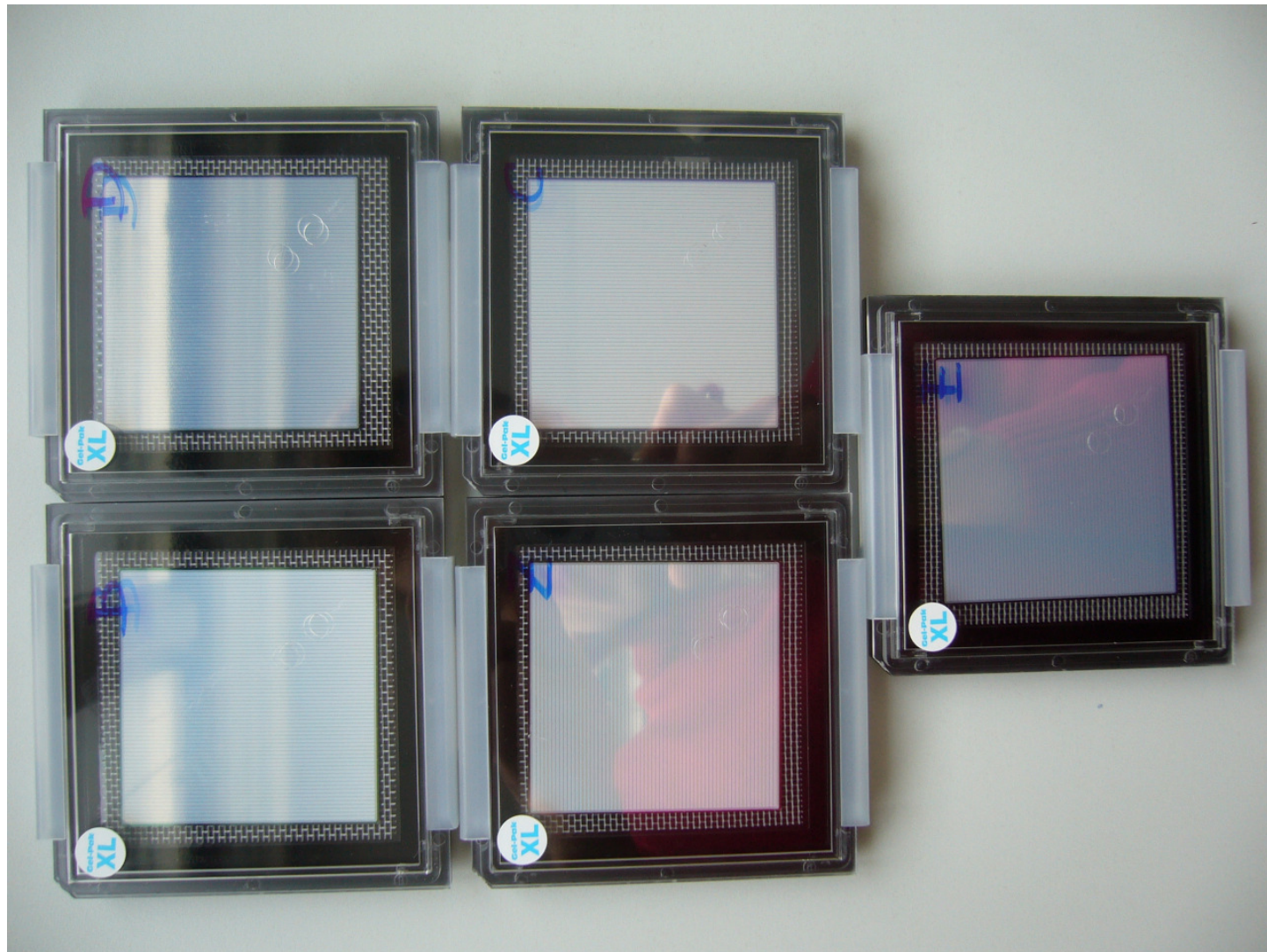
Operational reverse voltage limit: > 100 V

Impact from GSI tests:

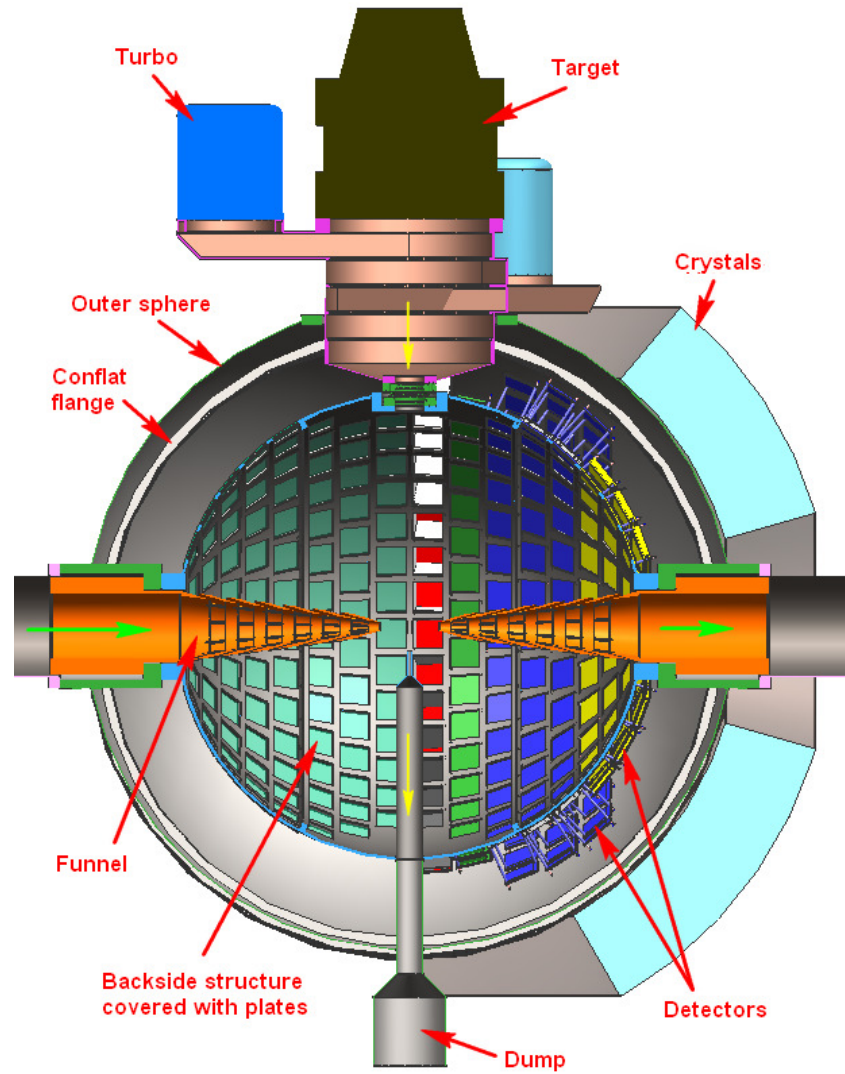
Improved p-side layout:

- P-side inplantation depth reduced
- Smaller contact stips at p-side
- Interstrip gap reduced to 10 µm

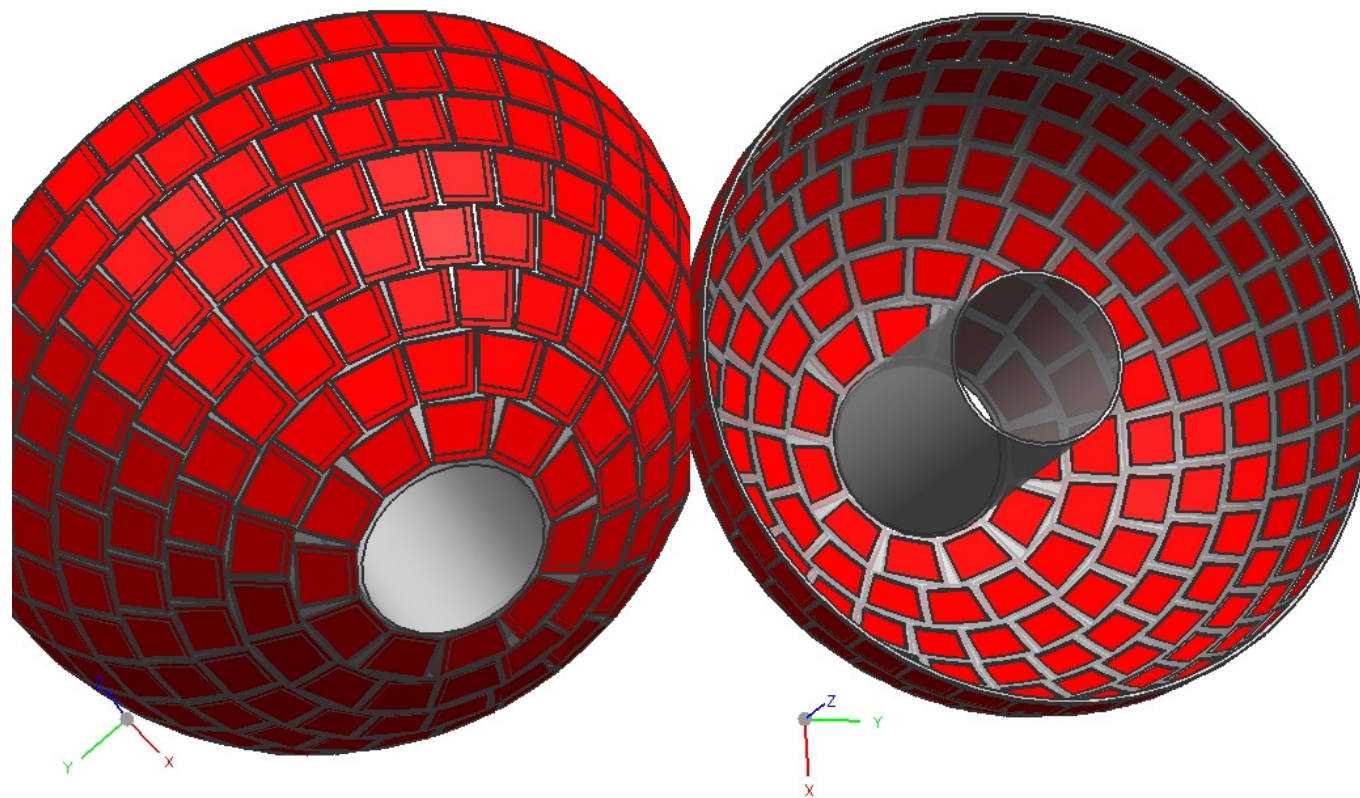
2nd Series of DSSD's from PTI St. Petersburg: 64 X 64 mm²



System Integration

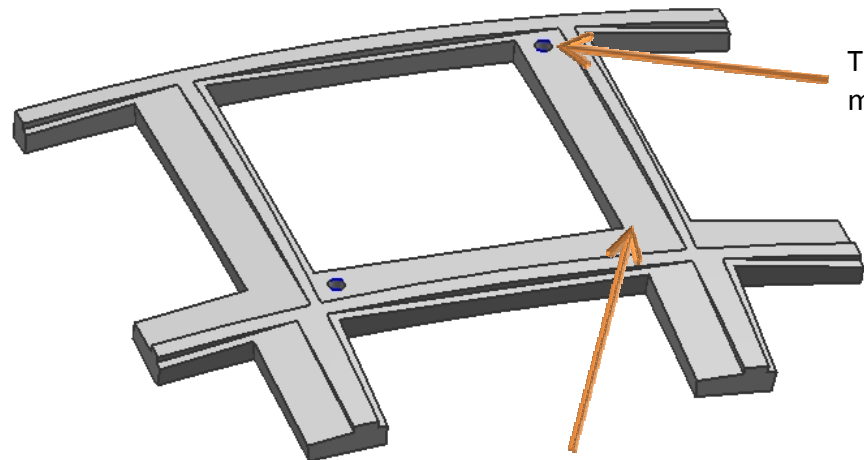


System Integration



Support Structure

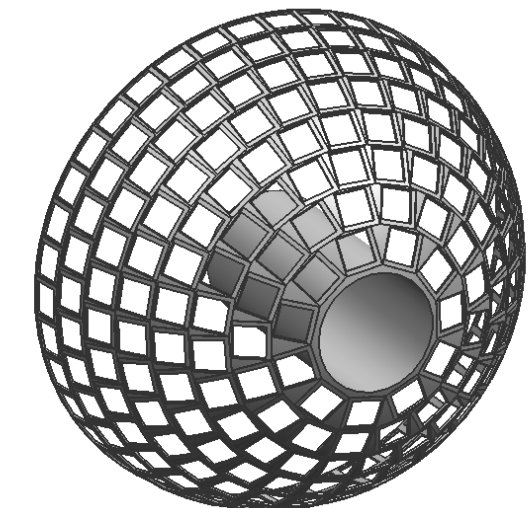
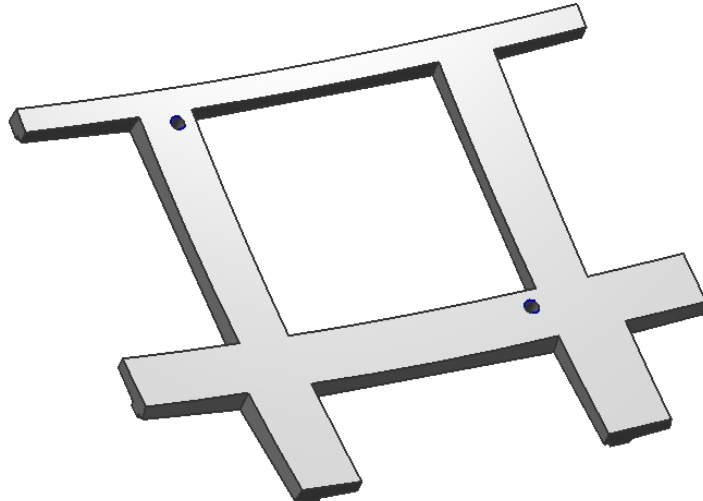
Outside



Flat cutouts to support detector and make it vacuum tight

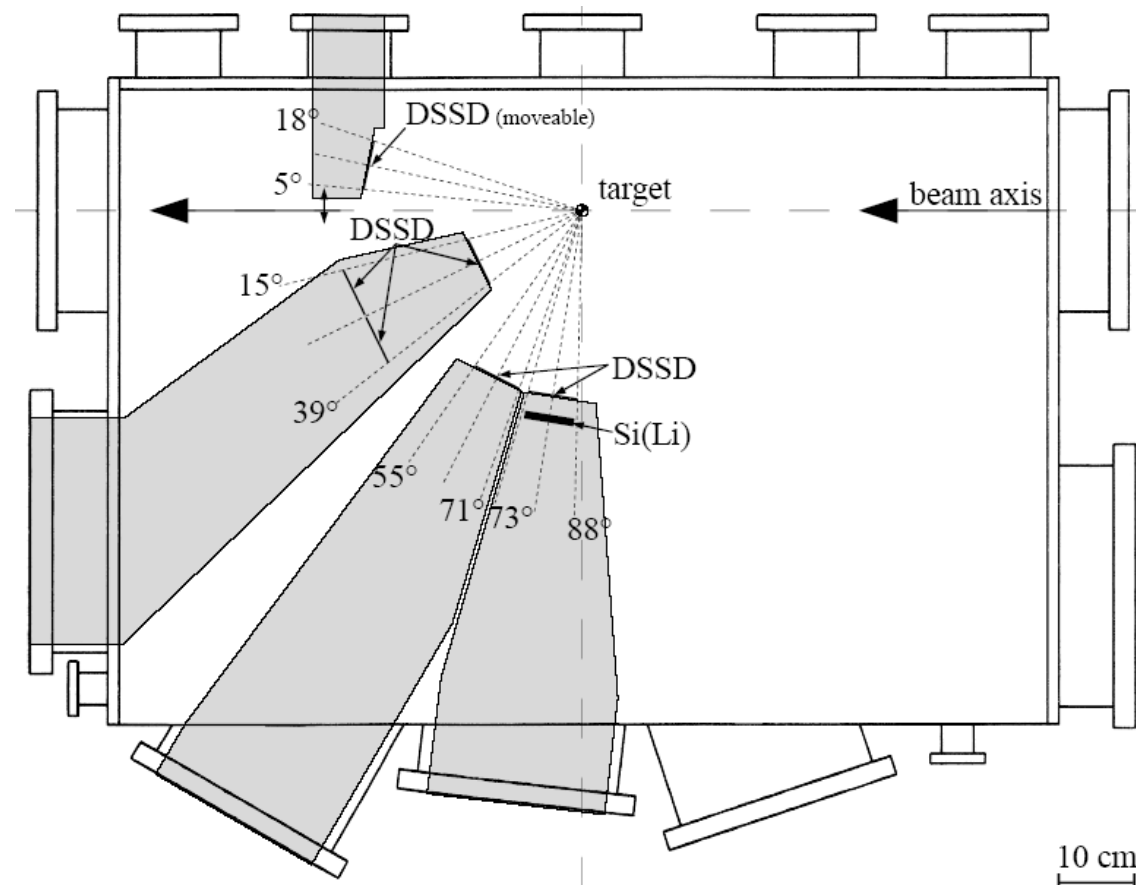
Thread holes for rods to mount detectors

Inside



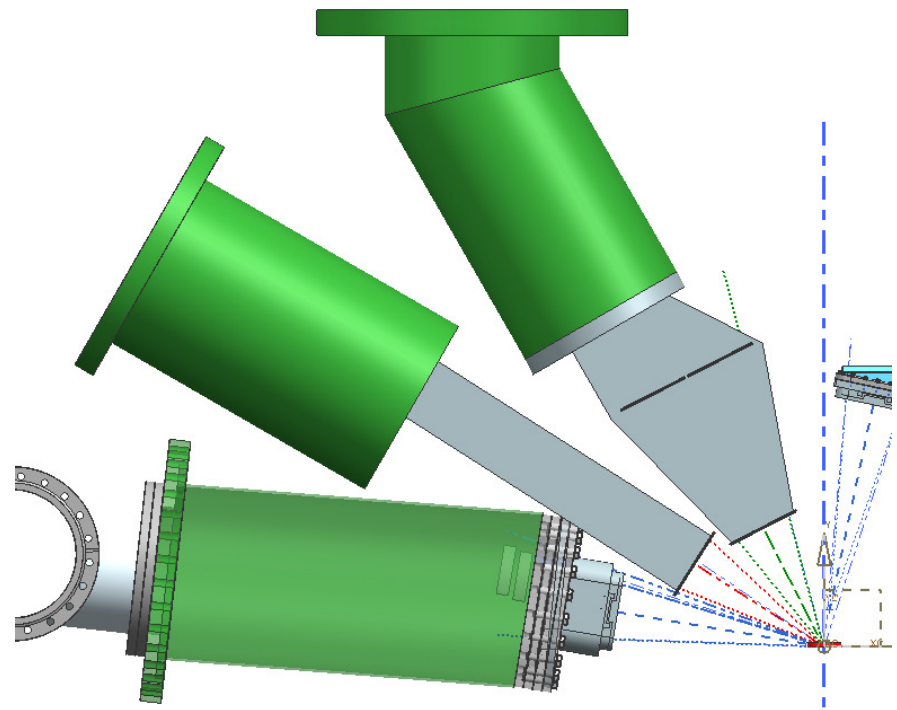
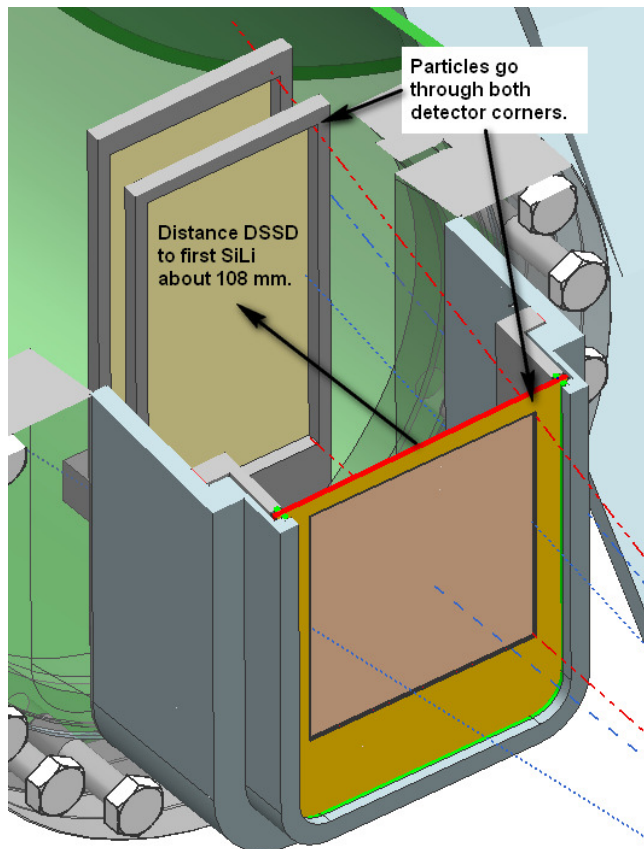
Proposal for Feasibility Studies and First Experiments with RIB's

(p,p), ($^3\text{He},\text{t}$), (α,α) reactions with ^{58}Ni and ^{56}Ni beams



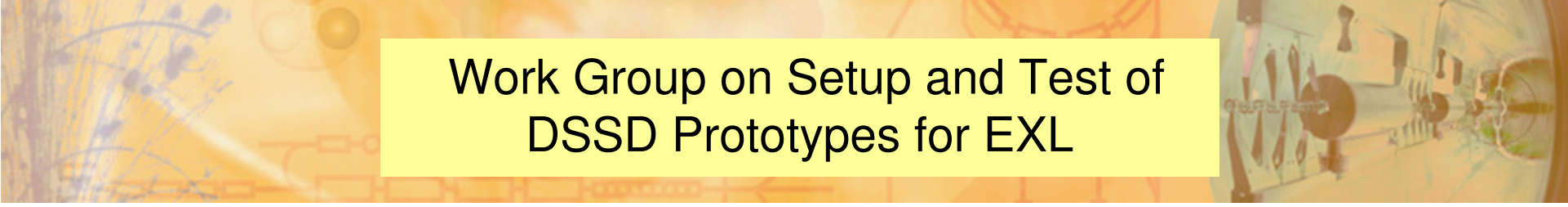
Design Study for First ESR Experiments

M. Lindemulder, KVI



Top view

DSSD – SiLi – SiLi telescope



Work Group on Setup and Test of DSSD Prototypes for EXL

R. Borger¹, T. Davinson², P. Egelhof³, V. Eremin⁴, S. Ilieva³
N. Kalantar¹, Y. Ke³, H. Kollmus³, T. Kröll⁶, X. C. Le³, M. Lindemulder¹,
M. Mutterer³, C. Rigollet¹, M. von Schmid⁶, B. Streicher⁵ P. Woods²

1 KVI Groningen

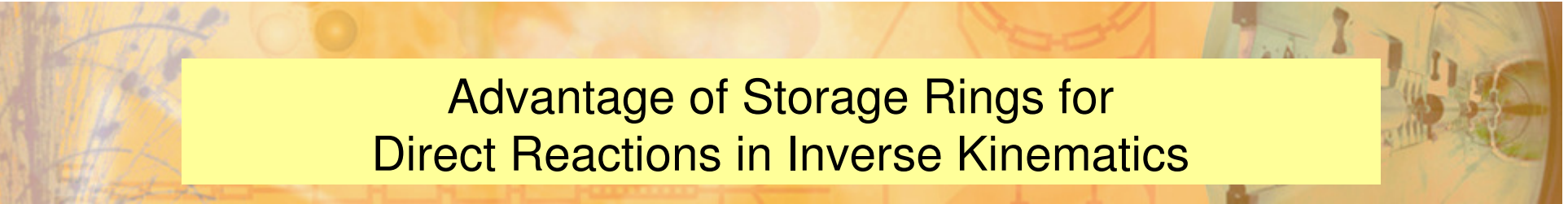
2 Univ. Edinburgh

3 GSI Darmstadt

4 PTI St. Petersburg

5 Univ. Mainz

6 TU Darmstadt



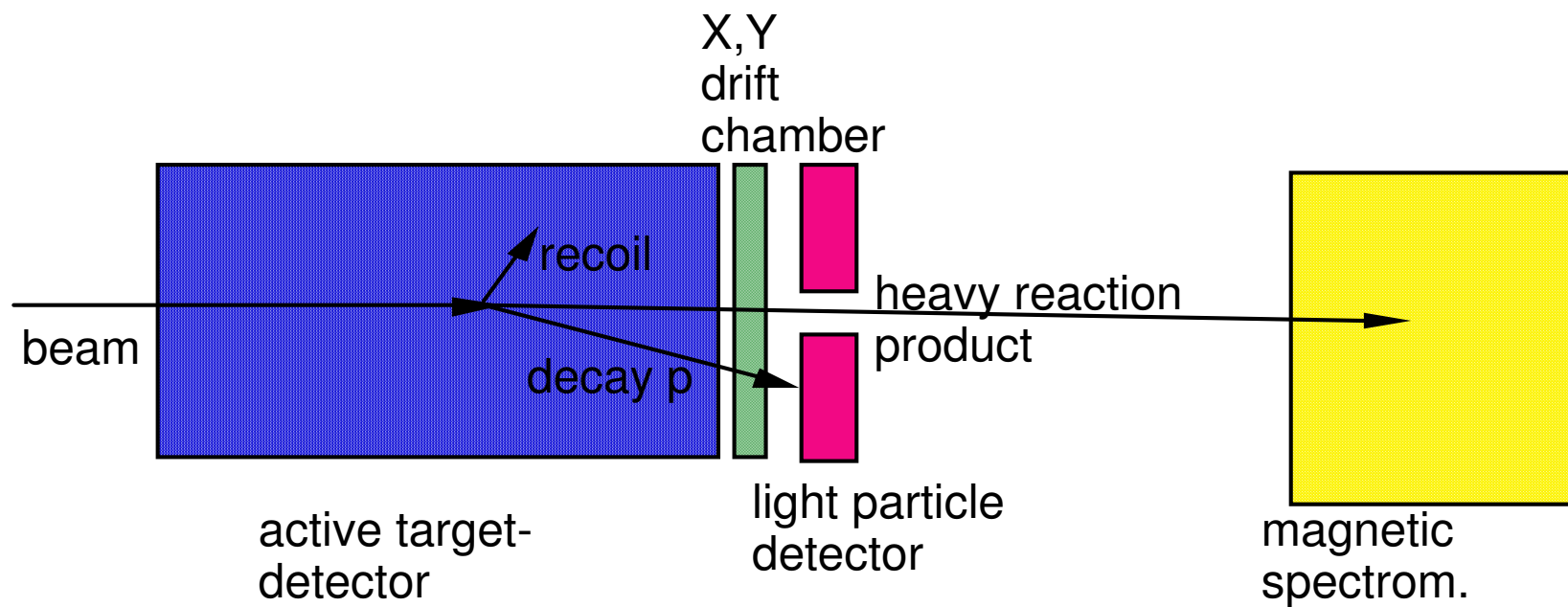
Advantage of Storage Rings for Direct Reactions in Inverse Kinematics

- gain of luminosity due to: continuous beam accumulation and recirculation
- high resolution due to: beam cooling, thin target
- low background due to: pure, windowless $^{1,2}\text{H}_2$, $^{3,4}\text{He}$, etc. targets
- separation of isomeric states

but: lifetime limit for very short lived exotic nuclei $T_{1/2} \geq 1$ sec

An Active Target for R³B

- ⇒ well suited as alternative technique to EXL for:
- short lifetimes ($T \leq 1$ sec)
 - low RIB intensities ($\leq 10^5$ sec⁻¹)





V. Conclusions

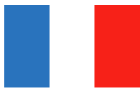
- elastic proton scattering at intermediate energies is a powerful tool to study nuclear matter distributions of halo nuclei
⇒ new data on ^{12}Be , ^{14}Be and ^{17}C
⇒ new data on charge radii in ^8He and ^{11}Li allow to deduce R_n and $R_n - R_p$
- the Future Facility NuSTAR@ FAIR will allow to reach unexplored regions in the chart of nuclei, where new and exciting phenomena are expected
- the EXL setup is designed as universal detection system providing high resolution and large luminosities for measurements at low momentum transfer
- the use of stored cooled radioactive beams within the EXL project will have considerable advantage over external target experiments in many cases



Univ. São Paulo



TRIUMF Vancouver



IPN Orsay, CEA Saclay



GSI Darmstadt, TU Darmstadt, Univ. Frankfurt, FZ Jülich, Univ. Mainz, Univ. Munich



INR Debrecen



SINP Kolkata



KVI Groningen



INFN/Univ. Milano



Univ. Osaka



JINR Dubna, Univ. St Petersburg, Moscow



CSIC Madrid, Univ. Madrid



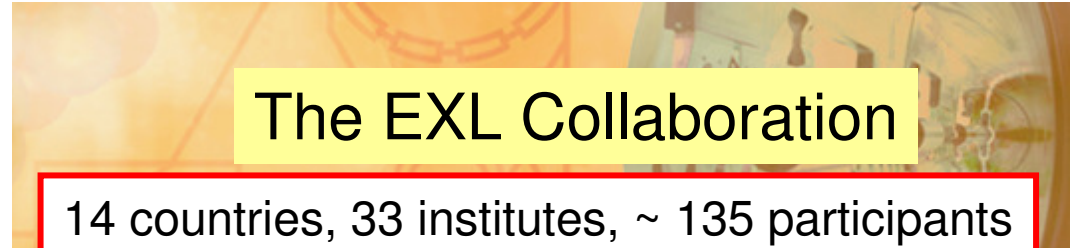
Univ. Lund, Mid Sweden Univ., TSL Uppsala

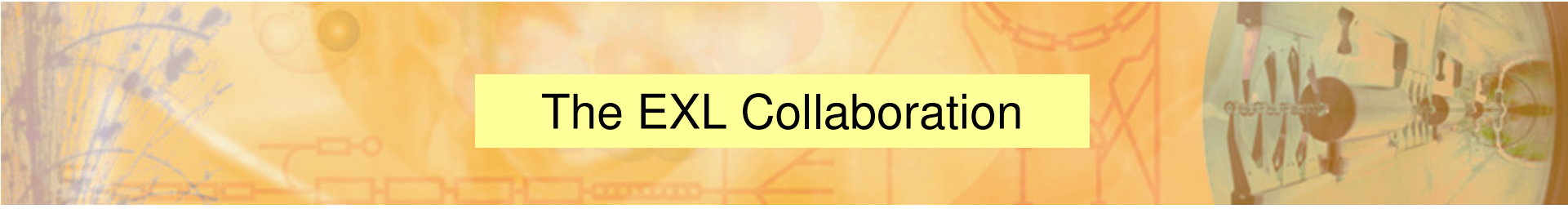


Univ. Basel



Univ. Birmingham, CLRC Daresbury, Univ. Surrey, Univ. York, Univ. Liverpool





The EXL Collaboration

Basel, Switzerland, Universität Basel - K. Hencken, B. Krusche, T. Rauscher, F. Thielemann

Birmingham, United Kingdom, University of Birmingham - M. Freer

Daresbury, United Kingdom, CLRC Daresbury Laboratory - P. Coleman-Smith, I. Lazarus, R. Lemmon, S. Letts, V. Pucknell

Darmstadt, Germany, Gesellschaft für Schwerionenforschung - T. Aumann, F. Becker, K. Beckert, K. Boretzky, A. Dolinski, P. Egelhof, H. Emling, H. Feldmeier, B. Franczak, H. Geissel, J. Gerl, S. Ilieva, C. Kozuharov, Y. Litvinov, T. Neff, F. Nolden, C. Peschke, U. Popp, H. Reich-Sprenger, H. Simon, M. Steck, T. Stöhlker, K. Sümerer, S. Typel, H. Weick, M. Winkler

Darmstadt, Germany, Technische Universität Darmstadt - G. Schriener

Debrecen, Hungary, Institute of Nuclear Research (ATOMKI) - A. Algara, M. Csátlos, Z. Gáski, J. Gulyás, M. Hunyadi, A. Krasznahorkay

Dubna, Russia, Joint Institute of Nuclear Research - A.G. Artukh, A. Fomichev, M. Golovkov, S.A. Klygin, G. A. Kononenko, S. Krupko, A. Rodin, Yu.M. Sereda, S. Sidorchuk, E. A. Shevchik, Yu.G. Teterev, A.N. Vorontsov

Frankfurt, Germany, Universität Frankfurt - R. Dörner, R. Grisenti, J. Stroth

Gatchina, Russia, St. Petersburg Nuclear Physics Institute and St. Petersburg State University - V. Ivanov, A. Khanzadeev, E. Rostchin, O. Tarasenkova, Y. Zalite

Göteborg, Sweden, Chalmers Institute - B. Jonson, T. Nilsson, G. Nyman

Groningen, KVI, The Netherlands - M. N. Harakeh, N. Kalantar-Nayestanaki, H. Moeini, C. Rigollet, H. Wörtche

Guildford, United Kingdom, University of Surrey - J. Al-Khalili, W. Catford, R. Johnson, P. Stevenson, I. Thompson

Jülich, Germany, Institut für Kernphysik, Forschungszentrum Jülich - D. Grzonka, T. Krings, D. Protic, F. Rathmann

Kolkata, India, Saha Institute of Nuclear Physics - S. Bhattacharya, U. Datta Pramanik

Liverpool, United Kingdom, University of Liverpool - M. Chartier, J. Cresswell, B. Fernandez Dominguez, J. Thornhill

Lund, Sweden, Lund University - V. Avdeichikov, L. Carlén, P. Gobulev, B. Jakobsson

Madrid, Spain, CSIC, Instituto de Estructura de la Materia - E. Garrido, O. Moreno, P. Sarriguren, J. R. Vignote, C. Martínez-Pérez, R. Alvarez Rodriguez, C. Fernandez Ramirez

Madrid, Spain, Universidad Complutense - L. Fraile Prieto, J. López Heraiz, E. Moya de Guerra, J. Udiá-Moinelo

Mainz, Germany, Johannes Gutenberg Universität - O. Kiselev, J.V. Kratz

Milan, Italy, Università da Milano and INFN - A. Bracco, P.F. Bortignon, G. Coló, A. Zalite

Moscow, Russia, Russian Research Centre, Kurchatov Institute - L. Chulkov

Mumbai, India, Bhabha Atomic Research Center - S. Kailas, A. Shrivastava

Munich, Germany, Technische Universität München - M. Böhmer, T. Faestermann, R. Gernhäuser, P. Kienle, R. Krücken, L. Maier, K. Suzuki

Orsay, France, Institut de Physique Nucléaire - D. Beaumel, Y. Blumenfeld, E. Khan, J. Peyre, J. Pouthas, J.A. Scarpaci, F. Skaza, T. Zerguerras

Osaka, Japan, Osaka University - Y. Fujita

São Paulo, Brasil, Universidade de São Paulo - A. Lépine-Szily

St. Petersburg, Russia, V. G. Khlopin Radium Institute - Y. Murin

St. Petersburg, Russia, Ioffe Physico-Technical Institute (PTI) - V. Eremin, Y. Tuboltcev, E. Verbitskaya

Sundsvall, Sweden, Mid Sweden University - G. Thungström

Tehran, Iran, University of Tehran - M. Mahjour-Shafiei

Uppsala, Sweden, The Svedberg Laboratory - C. Ekström, L. Westerberg

Vancouver, Canada, TRIUMF - R. Kanungo

